Monograph:
Zhou, B M, Wang, H.M. and Edwards, J.B. (1983) The Influence of Hydraulic Delay on the Composition Dynamics and Controller Design of Tray-Type Distillation Columns. Research Report. ACSE Report 209 . Department of Control Engineering, University of Sheffield, Mappin Street, Sheffield

THE INFLUENCE OF HYDRAULIC DELAY ON THE COMPOSITION DYNAMICS AND CONTROLLER DESIGN OF TRAY-TYPE DISTILLATION COLUMNS

by

B.M. Zhou*, H.M. Wang**, and J.B. Edwards

Department of Control Engineering,
University of Sheffield,
Mappin Street, Sheffield S1 3JD.

Research Report No. 209

January 1983

Senior Lecturer in Department of Control Engineering

*Visitor on leave from Shanghai Refinery, China

**Visitor on leave from Shaanxi Institute of Technology, China.

INTRODUCTION

It is essential for the design of controllers to know something of the dynamic characteristics of the plant concerned. The main method to obtain these characteristics at present is largely based on experimental analyses of existing plants. In a previous paper |1|, a useful analytical model for a symmetric binary distillation was deduced. Its transfer function matrix had a diagonal form and the elements of this matrix showed dynamic behaviour approaching that of a first order lag. These properties are significant for the controller design and plant design.

The present investigation, based on previous research |1|, involves the effect of hydraulic delay which, in practice, is not a negligible factor because it is evident that the liquid on one stage must take some time to flow down to another stage, in fact, the delay time takes the value from 1.0 second to 20 seconds for each stage |2|. Although the transfer function is very complicated and cannot be reformed into diagonal form, the inspection and analysis by the aid of computer indicate that the dynamic behaviour of all the elements of this matrix are still very near to that of a first order lag.

In the second part of this paper the authors design a set of controllers for this system using the dyadic expansion method |3|. The powerful interaction which exists between top and bottom products, is reduced with the proper choice of controllers, and it is obviously observed that even if the system without hydraulic delay has very high controller gain it can still keep stability while the system with hydraulic delay only a very low gain can be employed if instability is to be avoided.

1. MODELLING

1.1 Assumptions

(1) Equilibrium assumption:

Assume the column is operating under equilibrium condition. Then the composition of vapour and liquid should accord with the equilibrium relation shown in Fig 1. In the present instance, the equilibrium curve is approximated with two straight lines. These yield,

$$Y = X/\alpha + (\alpha-1)/\alpha \quad \text{in rectifier} \tag{1.1}$$

$$Y' = \alpha X' \quad \text{in stripper} \tag{1.2}$$

where the slope parameter is considered as a constant ($\alpha > 1.0$).

(2) Symmetric assumption:

As shown in the Fig. 2 it is assumed that the stage numbers in the rectifying section equals to those of the stripping section i.e. $N = N'$.

Also, the average molar flow of both vapour and liquid are assumed to be constant and have the following relations:

$$V_r = \alpha L_r \quad ; \quad L_s = \alpha V_s$$

$$V_r = L_s \quad ; \quad V_s = L_r \tag{1.3}$$

where the subscript r and s denote rectifying and stripping respectively.

(3) Feed assumptions:

The feed rate of vapour is assumed to equal to that of liquid i.e. $F_v = F_\ell = F$, and their composition are denoted by Y_F and X_F respectively. These yield

$$F = V_r - V_s$$

$$= V_r(1 - 1/\alpha) = V_r \cdot \varepsilon/\alpha \tag{1.4}$$

Furthermore, if the feed mixture is assumed to be in equilibrium, such that

$$Y_F = \alpha X_F$$

And the point (X_F, Y_F) will be the intersection of the minus 45^o line of equilibrium diagram with the equilibrium lines. That leads to:

$$Y_F = 1 - X_F$$

and $$Y_F = \alpha/(\alpha+1) \quad ; \quad X_F = 1/(\alpha+1) \tag{1.5}$$

(4) Vapour hold-up is neglected and the vapour flow on stages are equal to each other. The density of vapour is considered as a constant.

1.2 Total mass-flow balance for stage:

(1) For the rectifying section.

As shown in Fig. 3, the mass-flow balance is:

$$L_{n-1} - L_n + V_n - V_{n-1} = \dot{M}_n$$

According to the assumption $V_n = V_{n-1} = V$

so $$L_{n-1} - L_n = \dot{M}$$

For small sinusoidal signal:

$$\ell_{n-1} - \ell_n = j\omega\, m_n \tag{1.7}$$

where the notation $j\omega$ denotes the derivative operator.

The liquid hold-up is the function of liquid flow, vapour flow and vapour density.

$$M = f\{L,\ V/\sqrt{\rho_v}\ \}$$

Now that we assumed the vapour flow and density to be constant, we can write

$$\Delta M_n = \frac{\partial M}{\partial L}\ \Delta L_n$$

Or:

$$m_n = \tau_\ell . \ell_n \tag{1.8}$$

where $\tau_\ell = \partial M/\partial L$ is a hydraulic time constant.

Substituting (1.8) into (1.7) yields:

$$\ell_{n-1} - \ell_n = j\omega\tau_\ell . \ell_n \tag{1.9}$$

If the number of the stages are large enough we can use Taylor theorem and truncate the high order terms. Then equation (1.9) can be rewritten as

$$-\frac{d\ell}{dn} = j\omega\tau_\ell . \ell \tag{1.10}$$

Its solution is:

$$\log \frac{\ell_n}{c} = - j\omega\tau_\ell . \ell$$

Considering the boundary condition:

when n=o, $\ell_n = \ell_o$ (reflux) can decide the integral constant $c = \ell_o$.

So the final expression is

$$\ell_n = \ell_o . e^{-j\omega\tau_\ell . n} \qquad (1.11)$$

A similar expression can be deduced for the stripping section but note the stage order is from terminals to centre.

$$\ell_n = \ell_o . e^{-j\omega(2N+1 - n)\tau_\ell} \qquad (1.11)$$

Where the number n denotes the stage order in stripper. So it is evident from the above expressions that the difference between two liquid flows on different stages is only a time delay, and its value is in direct proportion to the distance from one stage to another.

1.3 Partial mass-flow balance:

(1) Small signal differential equation:

As shown in Figure 3 the mass flow balance in rectifying section is:

$$L_{n-1} X_{n-1} - L_n X_n + V_{n+1} Y_{n+1} - V_n Y_n = \frac{d}{dt} (M_n . X_n) \qquad (1.12)$$

For small sinusoidal signal

$$L_r x_{n-1} + \ell_{n-1} \bar{X}_{n-1} - L_r x_n - \ell_n \bar{X}_n + V_r y_{n+1} + v . \bar{Y}_{n+1} - V_r y_n - v \bar{Y}_n$$

$$= j\omega \bar{M} . x_n + j\omega m_n . \bar{X}_n$$

where the notation '-' denotes average value, and it is assumed that the average value of all parameters are constant. Rearranging the above equation can yield

$$- x_{n-1} + x_n - \frac{V_r}{L_r} y_{n+1} + \frac{V_r}{L_r} y_n + j\omega \frac{\dot{M}}{L_r} x_n$$

$$= \frac{1}{L_r} \left[\ell_{n-1} \bar{X}_{n-1} - (\ell_n + j\omega m_n) \bar{X}_n + v(\bar{Y}_{n+1} - \bar{Y}_n) \right] \qquad (1.13)$$

The equation (1.12) has the steady state form as following:

$$V_r (\bar{Y}_{n+1} - \bar{Y}_n) = (\bar{X}_n - \bar{X}_{n-1}) L_r \qquad (1.14)$$

Substituting (1.14) and (1.7) together with the assumptions of $V_r = \alpha L_r$ and $x = \alpha y$ into (1.13) yields:

$$- y_{n-1} + 2 y_n - y_{n+1} + j\omega T_x y_n = \frac{\bar{Y}_{n+1} - \bar{Y}_n}{V_r} \left| v - \alpha \ell_{n-1} \right| \quad (1.15)$$

where $T_x = \bar{M}/L_r$ is a time constant.

Again using Taylor theorem and substituting (1.11) into (1.15) can yield

$$\frac{\partial^2 y}{\partial n^2} - j\omega T_x y = \frac{\bar{Y}_n - \bar{Y}_{n+1}}{V_r} \left[v - \alpha \ell_o e^{-(n-1) j\omega \tau_\ell} \right] \quad (1.16)$$

For the sake of symmetry we assume $\bar{M}'/L_s = \bar{M}/L_r = T_x$ then a similar equation for stripping section is:

$$\frac{\partial^2 x'}{\partial n^2} - j\omega T_x x' = \frac{\bar{X}_{n+1} - \bar{X}_n}{V_r} \left[\alpha v - \ell_o e^{-(2N-n) j\omega \tau_\ell} \right] \quad (1.17)$$

(2) Steady State Version:

To solve the above differential equation, first we turn our attention to the steady state version of equation (1.12), we have

$$L_r \bar{X}_{n-1} - L_r \bar{X}_n + V_r \bar{Y}_{n+1} - V_r \bar{Y}_n = 0$$

With the relations of $V_r = \alpha L_r$ and $\bar{X} = \alpha \bar{Y} - (\alpha - 1)$ above equation can be simplified as:

$$\bar{Y}_{n-1} - 2 \bar{Y}_n + \bar{Y}_{n+1} = 0 \quad (1.18)$$

A similar equation for the stripping section is:

$$\bar{X}'_{n+1} - 2 \bar{X}'_n + \bar{X}'_{n-1} = 0 \quad (1.19)$$

the (1.18) and (1.19) are second order homogeneous difference equations, and have two repeated characteristic roots.

$$r_1 = r_2 = 1$$

So the solutions of these have the form as follows:

$$\left.\begin{aligned} \bar{Y}_n &= A_1 + A_2 n \\ \bar{X}'_n &= B_1 + B_2 n \end{aligned}\right\} \quad (1.20)$$

The constants can be decided by boundary conditions. For the top accumulator as shown in Fig. 3 the mass-flow balance is:

$$V(Y_1 - X_o) = \frac{d}{dt}(M_A X_o)$$

Its steady state form is

$$\bar{Y}_1 - \bar{X}_o = 0 \tag{1.21}$$

where M_A is the capacity of the accumulator.

Substituting the relation $\left[\bar{X}_o = \alpha \bar{Y}_o - (\alpha-1)\right]$ into (1.21) yields

$$\bar{Y}_1 = \alpha \bar{Y}_o - (\alpha-1) \tag{1.22}$$

Similarly we can get equations for the reboiler:

$$\bar{X}'_1 = \alpha \bar{X}'_o \tag{1.23}$$

As for the feed boundary condition, the steady state mass flow balance for the stage just above the feed point is:

$$FY_F + L_r \bar{X}_{N-1} - L_r \bar{X}_N + V_s \bar{Y}'_N - V_r \bar{Y}_N = 0 \tag{1.24}$$

And for the stage just below the feed point

$$FX_F + L_r \bar{X}_N - L_s \bar{X}'_N + V_s \bar{Y}'_{N-1} - V_s \bar{Y}'_N = 0 \tag{1.25}$$

Substituting the relations (1.3), (1.4) and (1.5) into Equation (1.24) and (1.25) and noticing $\bar{X} = \alpha \bar{Y} - (\alpha-1)$; $\bar{Y}' = \alpha \bar{X}'$ yields

$$\begin{aligned} \bar{Y}_{N-1} - 2\bar{Y}_N + \bar{X}'_N &= -\varepsilon/(\alpha+1) \\ \bar{X}'_{N-1} - 2\bar{X}'_N + \bar{Y}_N &= \varepsilon/(\alpha+1) \end{aligned} \tag{1.26}$$

Now substituting boundary conditions (1.22), (1.23) and (1.26) into (1.20) yields the solution:

$$\begin{aligned} \bar{Y}_n &= \bar{Y}_N + C(N-n) \\ \bar{X}'_n &= 1 - \bar{Y}_n \end{aligned} \tag{1.27}$$

where $C = 2\varepsilon/(\alpha+1)(2N\varepsilon + \alpha + 1)$ is the gradient of steady composition.

$$\bar{X}'_N = 1 - \bar{Y}_N = 2(N\varepsilon + 1)/(\alpha+1)(2N\varepsilon + \alpha + 1) \tag{1.28}$$

From (1.27) and (1.28) it is clear that

$$\bar{Y}_n - \bar{Y}_{n+1} = \bar{X}'_{n+1} - \bar{X}'_n = C \tag{1.29}$$

Substituting (1.29) into p.d.e (1.16) and (1.17) yields:

$$\frac{\partial^2 y}{\partial n^2} - py = \frac{C}{V_r}\left[v - \alpha \ell_o e^{-(n-1)pT_\ell}\right]$$

$$\frac{\partial^2 x'}{\partial n^2} - px' = \frac{C}{V_r}\left[\alpha v - \ell_o e^{-(2N-n)pT_\ell}\right] \qquad (1.30)$$

where $p = j\omega T_X$ and $T_\ell = \tau_\ell / T_X$

(3) Boundary conditions for small signal differential equations:

The mass-flow balance of top accumulator is:

$$V(Y_1 - Y_o) = \frac{d}{dt}(M_A X_o)$$

where M_A is the capacitance of accumulator which is a constant provided the level of accumulator is stable.

For small sinusoidal variations, above equation can be rewritten:

$$V_r(y_1 - x_o) + v(\bar{Y}_1 - \bar{X}_o) = j\omega M_A x_o$$

From (1.2) it is known that $\bar{Y}_1 - \bar{X}_o = 0$

So the above equation can be reduced to:

$$V_r(y_1 - x_o) = j\omega M_A x_o$$

Replacing y_1 by $(y_o + \partial y_o/\partial n)$ and using the relation $x = \alpha y$ can reduce the above euqation to:

$$-\varepsilon y_o + \frac{\partial y_o}{\partial n} = j\omega y_o T_A.$$

Or $\dot{y}_o = (\varepsilon + pT) y_o \qquad (1.31)$

where $\dot{y}_o = \left.\frac{\partial y}{\partial n}\right|_{n=o}$, $T_A = M_A/L_r$ is the residence time of accumulator

and

$$T = T_A/T_X \; ; \; p = j\omega T_X$$

Applying similar methods to the reboiler we get:

$$-\varepsilon x'_o + \frac{\partial x'_o}{\partial n} = j\omega x'_o T_A$$

or $\dot{x}'_o = (\varepsilon + pT) x'_o \qquad (1.32)$

where $T_B = M_B/L_s$ is the residence time of reboiler and for the sake of

symmetry we assume $T_B = T_A$

M_B is the capacitance of the reboiler which is a constant provided the level keeps stable.

Laplace transforming p.d.e (1.30) in s with respect to n get:

$$(s^2 - p)\tilde{y} - s\,y_o - \dot{y}_o = \frac{c}{V_r}\left[v/s - \alpha\,\ell_o e^{pT_\ell}/(s-pT_\ell)\right] \qquad (1.33)$$

$$(s^2 - p)\tilde{x}' - s\,x'_o - \dot{x}'_o = \frac{c}{V_r}\left[\alpha v/s - \ell_o e^{-2NpT_\ell}/(s-pT_\ell)\right]$$

The Laplace transform of Equations (1.31) and (1.32) is:-

$$\dot{y}_o = (\varepsilon + pT)\,y_o$$
$$\dot{x}'_o = (\varepsilon + pT)x'_o \qquad (1.34)$$

Substituting (1.34) into (1.33) to eliminate $\dot{y}_o$.

$$(s^2 - p)\tilde{y} - (s + \varepsilon + pT)y_o = \frac{c}{V_r}\left|v/s - \alpha\,\ell_o e^{pT_\ell}/(s) + pT_\ell)\right|$$
$$(s^2 - p\,\tilde{x}' - (s + \varepsilon + pT)x'_o = \frac{c}{V_r}\left|\alpha\,v/s - \ell_o\,e^{-2NpT_\ell}/(s-pT_\ell)\right. \qquad (1.35)$$

Rearranging both sides of (1.35)

$$\tilde{y} = \frac{s + \varepsilon + pT}{s^2 - p}\,y_o + \frac{c}{V_r}\left(\frac{v}{s(s^2 - p)} - \frac{\alpha\,\ell_o\,e^{pT_\ell}}{(s + pT_\ell)(s^2 - p)}\right)$$
$$\tilde{x}' = \frac{s + \varepsilon + pT}{s^2 - p}\,\tilde{x}'_o + \frac{c}{V_r}\left(\frac{\alpha\,v}{s(s^2-p)} - \frac{\ell_o\,e^{-2NpT_\ell}}{(s - pT_\ell)(s^2-p)}\right) \qquad (1.36)$$

Inverse Laplace transforming (1.36) into n domain leads to:

$$y_n = \left[\cosh\sqrt{p}\,n + \frac{\varepsilon+pT}{\sqrt{p}}\sinh\sqrt{p}\,n\right]y_o - \frac{c}{V_r}\cdot\frac{v}{p}\left[1 - \cosh\sqrt{p}\,n\right]$$
$$+ \frac{c}{V_r}\,\frac{\alpha\cdot\ell_o}{p-p^2T_\ell^2}\left(e^{-(n-1)pT_\ell} + \frac{pT_\ell\,e^{pT_\ell}}{\sqrt{p}}\sinh\sqrt{p}\,n - e^{pT_\ell}\cosh\sqrt{p}\,n\right) \qquad (1.37)$$

$$x'_n = \left[\cosh\sqrt{p}\,n + \frac{\varepsilon+pT}{\sqrt{p}}\cdot\sinh\sqrt{p}\,n\right]x'_o - \frac{c}{V_r}\,\frac{\alpha v}{p_1}\left[1 - \cosh\sqrt{p}\,n\right]$$
$$+ \frac{c}{V_r}\,\frac{\ell_o}{p-p^2T_\ell^2}\left(e^{-(2N-n)pT_\ell} - \frac{pT_\ell\,e^{-2NpT_\ell}}{\sqrt{p}}\sinh\sqrt{p}\,n - e^{-2NpT_\ell}\cosh\sqrt{p}\,n\right) \qquad (1.38)$$

Now turning the attention to the feed boundary condition. We first take the partial mass-flow balance of the stage just above the feed point.

$$FY_F + L_{N-1}X_{N-1} - L_N X_N + V'_N Y'_N - V_N Y_N = \frac{d}{dt}(M_N X_N)$$

For the small sinusoidal perturbation the above equation becomes:

$$L_r x_{N-1} + \ell_{N-1}\bar{X}_{N-1} - L_r x_N - \ell_N \bar{X}_N + V_s y'_N + v\bar{Y}'_N - V_r y_N - v\bar{Y}_N = \bar{M}j\omega x_N + j\omega m_N \bar{X}_N$$

Using relations $V_s = L_r$ and $x_N = \alpha y_N$ it reduces to:

$$V_r(x'_N - y_N) + V_r(y_{N-1} - y_N) - j\omega x_N \bar{M}$$

$$= (\ell_N + j\omega m_N)\bar{X}_N - v(\bar{Y}'_N - \bar{Y}_N) - \ell_{N-1}\bar{X}_{N-1} \qquad (1.39)$$

According to the equation (1.7) we have

$$\ell_N + j\omega m_N = \ell_{N-1}$$

and substituting it into equation (1.39) then using Taylor theorem the equation (1.39) reduces to

$$x'_N - y_N - \dot{y}_n - p\, y_N = \frac{-v}{V_r}(\alpha\bar{X}'_N - \bar{Y}_N) - \frac{\alpha\ell_{N-1}}{V_r}(\bar{Y}_{N-1} - \bar{Y}_N)$$

The above equation can be further reduced by using relations (1.28) and (1.29)

$$x'_N - y_N - \dot{y}_N - py_N = \frac{C}{V_r}\left[\frac{\alpha+1}{2}\cdot v - \alpha\,\ell_o\, e^{-(N-1)pT_\ell}\right] \qquad (1.40)$$

Applying similar method to the stage just below the feed point can get similar equation

$$y_N - x'_N - \dot{x}'_N - px'_N = \frac{C}{V_r}\left[\alpha v - \frac{\alpha+1}{2}\,\ell_o e^{-NpT_\ell}\right] \qquad (1.41)$$

Differentiating equation (1.37) and (1.38) and replacing n by N so that to get $\dot{y}_N$ and $\dot{x}'_N$:

$$\dot{y}_N = \left[\sqrt{p}\ \sinh\sqrt{p}N + (\varepsilon+pT)\ \cosh\sqrt{p}N\right] y_o + \frac{c}{V_r} \cdot \frac{v}{p}\sqrt{p}\ \sinh\sqrt{p}\ N$$

$$+ \frac{c}{V_r}\ \frac{\alpha \ell_o}{p-p^2T^2}\left[-pT_\ell e^{-(N-1)pT_\ell} + pT_\ell\ e^{pT_\ell}\cosh\sqrt{p}\ N - \sqrt{p}\ e^{pT_\ell}\sinh\sqrt{p}N\right] \tag{1.42}$$

$$\dot{x}'_N = \left[\sqrt{p}\ \sinh\sqrt{p}N + (\varepsilon+pT)\ \cosh\sqrt{p}N\right] x'_o + \frac{c}{V_r}\ \frac{\alpha v}{p}\sqrt{p}\ \sinh\sqrt{p}\ N$$

$$+ \frac{c}{V_r}\ \frac{\ell_o}{p-p^2T_\ell^2}\left[pT_\ell e^{-NpT_\ell} - pT_\ell e^{-2NpT_\ell} \cdot \cosh\sqrt{p}N - \sqrt{p}e^{-2NpT_\ell}\sinh\sqrt{p}N\right] \tag{1.43}$$

1.4 Solution

Now substituting (1.37), (1.42) and (1.38), (1.43) into (1.40) and (1.41) respectively can yield the expressions of y_o and x'_o, but it will be very complicated and some notations must be introduced so that to make the results brief.

$$\phi x'_o = \left[(1+p)\phi + \phi'\right] y_o + \phi_1 \frac{c}{V_r}\ell_o + \phi_2 \frac{c}{V_r} v$$

$$\phi y_o = \left[(1+p)\phi + \phi'\right] x'_o + \phi_3 \frac{c}{V_r}\ell_o + \phi_4 \frac{c}{V_r} v \tag{1.44}$$

where

$$\phi = \cosh\sqrt{p}\ N + \frac{\varepsilon + pT}{\sqrt{p}}\ \sinh\sqrt{p}\ N$$

$$\phi' = \sqrt{p}\ \sinh\sqrt{p}\ N + (\varepsilon + pT)\ \cosh\sqrt{p}N$$

$$\phi_1 = \left[(1 + p^2T_\ell^2 - p\ T_\ell)\alpha . e^{-(N-1)pT_\ell} - e^{-NpT_\ell} + \right.$$

$$+ \alpha(1+p)e^{pT_\ell}\left(\frac{e^{pT_\ell}}{\sqrt{p}}\sinh\sqrt{p}\ N - \cosh\sqrt{p}\ N\right)$$

$$+ \alpha e^{pT_\ell}.(pT_\ell\cosh\sqrt{p}N - \sqrt{p}\ \sinh\sqrt{p}\ N) +$$

$$\left. + e^{-2NpT_\ell}\left(\frac{e^{pT_\ell}}{\sqrt{p}}\sinh\sqrt{p}\ N + \cosh\sqrt{p}\ N\right)\right] / (p - p^2\ T_\ell^2)$$

$$\phi_2 = \left[\sqrt{p}\,\sinh\sqrt{p}N - (1+p-\alpha)(1-\cosh\sqrt{p}N) + \frac{\alpha+1}{2}p\right]/p$$

$$\phi_3 = \left[(1+p+pT_\ell)e^{-NpT_\ell} - \alpha e^{-(N-1)pT_\ell} + \alpha e^{pT_\ell}\cdot\right.$$
$$\cdot\left(\cosh\sqrt{p}N - \frac{pT_\ell}{\sqrt{p}}\sinh\sqrt{p}\,N\right)$$
$$- (1+p)e^{-2NpT_\ell}\cdot\left(\frac{e^{pT_\ell}}{\sqrt{p}}\sinh\sqrt{p}N + \cosh\sqrt{p}N\right) - e^{-2NpT_\ell}\cdot$$
$$\cdot\left(pT_\ell\cosh\sqrt{p}N + \sqrt{p}\,\sinh\sqrt{p}\,N\right)$$
$$\left. - \frac{\alpha+1}{2}(p-p^2T_\ell^2)e^{-NpT_\ell}\right]/(p - p^2T_\ell^2)$$

$$\phi_4 = \left[(1-\alpha-\alpha p)(1-\cosh\sqrt{p}\,N) + \alpha\sqrt{p}\,\sinh\sqrt{p}\,N + \alpha p\right]/p$$

The final expressions of y_o and x'_o are:

$$A = G\,F \tag{1.45}$$

where:

$A = \begin{pmatrix} y_o \\ x'_o \end{pmatrix}$ is the composition vector

$F = \begin{pmatrix} \ell_o \\ v \end{pmatrix} \cdot \frac{c}{V_r}$ is the flow vector

$$G = \begin{pmatrix} -(1+p)\phi-\phi' & \phi \\ \phi & -(1+p)\phi-\phi' \end{pmatrix}^{-1} \begin{pmatrix} \phi_1 & \phi_2 \\ \phi_3 & \phi_4 \end{pmatrix}$$

G is called the transfer function matrix or T.F.M. for short

The results are very tedious, but when either p or T_ℓ leads to zero it will be the same as those in reference [1]. In fact, the factor e^{-pT_ℓ} leads to 1 as $pT_\ell \to 0$, and in this case the T.F.M. can be reduced to diagonal form just the same as the results in reference [1].

If we define

$$Q = \begin{pmatrix} y_o - x'_o \\ y_o + x'_o \end{pmatrix} \quad \text{and} \quad D = \begin{pmatrix} v + \ell_o \\ v - \ell_o \end{pmatrix} \frac{c}{V_r}$$

$$G' = \begin{pmatrix} g'_{11} & g'_{12} \\ g'_{21} & g'_{22} \end{pmatrix}$$

$$\begin{aligned} g'_{11} &= 0.5(g_{11} + g_{12} - g_{21} - g_{22}) \\ g'_{12} &= 0.5(g_{12} - g_{11} + g_{21} - g_{22}) \\ g'_{21} &= 0.5(g_{11} + g_{12} + g_{21} + g_{22}) \\ g'_{22} &= 0.5(g_{12} - g_{11} - g_{21} + g_{22}) \end{aligned} \tag{1.46}$$

where:

g_{11}, g_{12}, g_{21} and g_{22} are the elements of matrix G.

As $pT = 0$, $g_{12} = -g_{21}$ and $g_{22} = -g_{11}$

Then we can write:

$$Q = G' \cdot D \tag{1.47}$$

In the case of $pT_\ell = 0$. $g'_{12} = g'_{21} = 0$ i.e. the matrix G' is diagonal, and the elements of this diagonal matrix are:

$$\begin{aligned} g'_{11} &= (\varepsilon N^2 + \varepsilon N + 0.5\varepsilon)/(2\varepsilon N + \alpha + 1) \\ g'_{22} &= \left[(\alpha+1)N + 0.5(3\alpha + 1)\right]/\varepsilon \end{aligned} \tag{1.48}$$

These results are all the same as those in reference |1|

In general case G' is not a diagonal matrix and the off-diagonal elements are not negligible.

2. CONTROLLER DESIGN

To design the forward-path controller, the 'dyadic Expansion' method |3| is used here. The important feature of this metod is that it enables systematic compensation of characteristic loci by independent choice of proper scalar transfer functions of the controller.

2.1 Dyadic Approximation of Systems

As distillation columns systems are of quite complicated structures, it is difficult to get a dyadic approximation form by means of analysis.

Therefore, choose an interesting high frequency ω_1, for example 0.2, (it is high enough because their corner frequencies about equal to 0.065) and write

$$G(i\omega_1) = A_1 + i\, A_2$$

Where A_1 and A_2 are real 2x2 matricies. for $\omega_1 = 0.2$

$$A_1 = \begin{pmatrix} -0.441 & 0.345 \\ -2.764 & 0.398 \end{pmatrix} \qquad A_2 = \begin{pmatrix} -3.463 & 3.337 \\ -2.271 & 3.695 \end{pmatrix}$$

It is easy to prove that if A_1 is nonsingular and $A_2 A_1^{-1}$ has a nonsingular eigenvector matrix W and eigenvalues λ_j, j = 1,2 then

$$G(i\omega_1) = W\, \mathrm{diag}\{1 + i\lambda_j\} W^{-1} A_1 \tag{2.1}$$

i.e. G(p) can be transformed into diagonal form by W and $W^{-1}A_1$ in $p = i\omega$, point

$$\text{When } \omega_1 = 0.2 \qquad W = \begin{pmatrix} 1 & 1 \\ 34.79 & 1.108 \end{pmatrix}$$

$$\text{Define } H(p,\omega_1) = W^{-1}(\omega_1) G(p) U(\omega_1) \tag{2.2}$$

$$\text{where} \qquad U(\omega_1) = A_1^{-1} W = \begin{pmatrix} -14.8 & 0.005 \\ -15.6 & 2.818 \end{pmatrix} \quad \omega_1 = 0.2$$

According to continuity, $H(p,\omega_1)$ is of approximately diagonal form over the range of frequencies in the vicinity of ω_1. The validity of this approximation can be investigated by obtaining the plot of $g_j(i\omega,\omega_1)$ (the diagonal terms of $H(i\omega,\omega_1)$ and superimposing the Gershgorin circles with radii

$$\gamma_j(i\omega,\omega_1) = \left| H_{\ell j}(i\omega,\omega_1) \right|_{\ell \neq j} \tag{2.3}$$

in it.

Sometimes, the range of frequencies may appear to be small, but it can be improved by scaling the rows of $H(i\omega,\omega_1)$, i.e. write

$$G(p) = W\,\mathrm{diag}\{u_j\}\mathrm{diag}\{\frac{1}{u_j}\}\ H(p,\omega_1)W^{-1}A_1 \tag{2.4}$$

and regard $\mathrm{diag}\{\frac{1}{u_j}\}\ H(p,\omega_1)$ as $H(p,\omega_1)$

In our case, choose $\mathrm{diag}\{\frac{1}{u_j}\} = \begin{pmatrix} 1 & 0 \\ 0 & \frac{1}{10} \end{pmatrix}$, and their plots are shown in Fig. 6.

It can be seen from Fig. 6 that fractional error is less than 0.5 over the range of frequencies 0.05 - 1.0. This is wide enough for controller design purposes.

2.2 Controller Design

Set the forward-path controller to be of the form

$$K(p) = K(p,\omega_1) = A_1^{-1}\,W\ \mathrm{diag}\ \{k_j(p,\omega_1)\}_{j=1,2}\ \mathrm{diag}\{\frac{1}{u_j}\}W^{-1} \tag{2.5}$$

Where $k_j(p,\omega_1)$ are proper scalar minimum-phase compensation elements.

Forward-path transfer function matrix is

$$G(p)K(p) = W\ \mathrm{diag}\{u_j\}\mathrm{diag}\ \{\frac{1}{u_j}\}H(p,\omega_1)\mathrm{diag}\{k_j(p,\omega_1)\}\mathrm{diag}\{\frac{1}{u_j}\}W^{-1} \tag{2.6}$$

The closed-loop transfer function matrix is

$$H_c(p) = \{I_2 + G(p)\ K(p)\}^{-1}G(p)K(p)$$

$$\simeq W\ \mathrm{diag}\ \{u_j\}\mathrm{diag}\{\frac{g_jk_j}{1+g_jk_j}\}\mathrm{diag}\{\frac{1}{u_j}\}W^{-1} \tag{2.7}$$

(by neglecting the off-diagonal terms in $H(p,\omega_1)$)

so

$$H_c(p) \simeq W\ \mathrm{diag}\ \{\frac{g_jk_j}{1+g_jk_j}\}\ W^{-1} \tag{2.8}$$

Choose $k_j(p,\omega_1)$ such that

1) Closed-loop system is stable and g_jk_j have the desired gain and phase margins.

2) $g_1k_1 \simeq g_2k_2$ over the frequency range of interest (in order to reduce their interaction).

Through a lot of computing, the final $\text{diag}\{k_j(p,\omega_1)\}$ choice is

$$\text{diag}\{k_j(p,\omega_1)\} = \begin{bmatrix} 2 & 0 \\ 0 & -1.2(1+10p) \end{bmatrix}$$

The plots of $g_j(i\omega,\omega_1)k_j(i\omega,\omega_1)$ are shown in Fig. 7. Their Gershgorin Circles are superimposed in the same Fig. 7. The plots and their Gershgorin Circles do not encircle (-1,0) point, so the closed-loop system is stable.[3] Furthermore, the phase margin and gain margin are 62° and 3.9 respectively for g_1k_1. For g_2k_2, the phase margin is 145° and the gain margin is infinity.

The controller transfer function matrix is

$$K(p) = A_1^{-1}W \begin{bmatrix} 2 & 0 \\ 0 & -1.2(1+10p) \end{bmatrix} \begin{bmatrix} 1 & 0 \\ 0 & \frac{1}{10} \end{bmatrix} W^{-1}$$

$$= \begin{bmatrix} 0.976 - 0.006p & -0.881 \\ 0.678 - 35p & -0.916 + 0.1p \end{bmatrix} \qquad (2.9)$$

3.3 Investigation of interaction

At high frequency, for example, $0.1 < \omega < 0.3$, it can be seen from Fig. 7 that

$$g_1(i\omega,\omega_1)k_1(i\omega,\omega_1) \simeq g_2(i\omega,\omega_1)k_2(i\omega,\omega_1)$$

Then from (2.8) we can write closed-loop T.F.M. as

$$H_c(p) \simeq \frac{g_1(i\omega,\omega_1)k_1(i\omega,\omega_1)}{1+g_1(i\omega,\omega_1)k_1(i\omega,\omega_1)} I_2 \qquad (2.10)$$

This formula roughly indicates that interaction effects are small over the frequency range of 0.1 - 0.3.

At very low frequencies, we use the decomposition

$$H_c(p) = \{I_2 + Q(p)\}^{-1} Q(p)$$

$$= V^{-1}(p)\ \mathrm{diag}\{\frac{q_j(p)}{1+q_j(p)}\}_{j=1,2}\ V(p) \qquad (2.11)$$

Where q_j are eignevalues of $Q(p)$, and $V(p)$ is eigenvector matrix of $Q(p)$

For our system, when $\omega = 0.01$

$$H_c(p) = V^{-1}(p) \begin{bmatrix} \frac{4.6-0.78i}{1+(4.6-0.78i)} & 0 \\ 0 & \frac{12.28-16.36i}{1+(12.28-16.36i)} \end{bmatrix} V(p) \qquad (2.12)$$

$\therefore |q_j| \gg 1 \quad \therefore H_c(p) \simeq I_2$

That means the interaction effects are also small when $0 < \omega < 0.01$.

Of course, interaction effects still exist. Exact decoupling controller design requires special study.

2.4 Compare with $T_\ell = 0$ case

The forward-path controller can be designed by some way for $T_\ell = 0$ case. For simplicity, we discuss proportional control only. In $T_\ell = 0$ case, controller can have very high gain and closed-loop system is still stable. For example when

$$K(p) = \begin{bmatrix} 46.5 & -46.3 \\ 46.3 & -45.5 \end{bmatrix}$$ the plots of $g_j(i\omega,\omega_1)k_j(i\omega,\omega_1)$ are shown in Fig. 8.

But for $T_\ell = 0{,}2$ case . When $K = \begin{bmatrix} 2.92 & -2.64 \\ 2.73 & -2.76 \end{bmatrix}$, closed-loop system is near unstable. The plots are shown in Fig. 9.

|1| pointed, when $T_\ell = 0$, plant can be regarded as first-order type systems, i.e. its T.F.M. can be written as

$$G(p) = \{A_o p + A\}^{-1} \qquad (2.13)$$

where A_o and A are constant matrices.

In |3|, Owens points out that, for first-order type systems, if we choose a forward-path controller $K(p) = k\ A_o - A$ then one can easily prove that the system is asymptotically stable if and only if $k>0$. This means one can set the gain value arbitrarily large. The above example illustrates however that, when time delay is present, the gain must not be set too high. In other words, time delay can cause instability even when occuring in conjunction with first order type systems.

Discussion and Conclusion:

Although the T.F.M. has a very complicated form, the Bode diagrams show that the dynamic characteristics of all elements of T.F.M. is very near to first order lag (Fig. 4), and the fact that their phase lags exceed 90^o shows this system to be non-minimum phase. A better way to approximate the system is therefore to use a first order lag in series with a dead time lag. For the sake of comparison, Fig. 4 shows the Bode diagrams for both systems with and without hydraulic delay makes negligible difference to the elements of T.F.M. with the exception of g_{21} whose phase angle at high frequency shows big difference increasing with frequency. This change of phase angle can be expressed as the difference of dead time, as following:

$$|g_{21}|_{T_\ell > 0} = k.|g_{21}|_{T_\ell = o} . e^{-\Delta\tau.p}$$

where: $\Delta\tau$ is the difference of dead time between $T_\ell > 0$ and $T_\ell = 0$

p is Laplace operator.

Using Least Square Method at $T_\ell = 0.2$ and within the frequency range from 0.0001 to 1.0 gets the results as follows:

$$k = 1.0\ ;\ \Delta\tau = 3.76 \simeq 0.2 * 20$$

and the error is very little.

These results show that the hydraulic delay mainly effects the dead time of elements g_{21} of T.F.M.

From the technological point of view, g_{11} is the response of top omposition y_o to reflux ℓ_o and because the reflux point is very near to the distillate point, the hydraulic delay only has a small influence on g_{11} while g_{21} is the response of bottom composition x'_o to reflux ℓ_o and there are (2N+1) stages between reflux point and bottom so the influence of hydraulic delay is obvious. Similarly, for g_{12} and g_{22}, because it is assumed that the vapour flow involves no time delay, they are independent of hydraulic delay, and from the above discussion, we can reasonably suppose that if the vapour hydraulic delay is taken into account, it will mainly influence the dead time of g_{12} of T.F.M.

The forward-path controller is designed using 'Dyadic Expansion Method' This paper also demonstrates that hydraulic delay has an obvious influence on system stability and controller design. Dead time lag can cause instability when it occurs in conjunction even with first order type systems.

References

|1| Edwards, J.B., and Tabrizi, M.H.N., 'An analytically-derived, parametric transfer-function model for ideal tray-type, binary distillation columns', University of Sheffield, Dept. of Control Eng., Research Report No.

|2| Rademaker, O., Rijnsdorp, J.E., and Mearleveld, A.,'Dynamics and Control of continuous distillation units', (Amsterdam-Oxford- New York, 1975).

|3| Owens, D.H., 'Feedback and multivariable systems' (Peter Peregrimus, 1978)

|4| Edwards, J.B., and Jassim, H.J., 'An analytical study of the dynamics of binary distillation columns' (TRANS, Inst. Chem. Engrs., Vol.55, 1977).

List of Symbols

α	- initial slope of equilibrium curve approximation
ε	- $\alpha - 1$
F	- molar feed rates of liquid and vapour
c	- spatial steady state composition gradient
G	- transfer function matrix (T.F.M.)
$g_{11}, g_{12}, g_{21}, g_{22}$	- the elements of T.F.M.
L_r, L_s, ℓ	- molar flow of liquid in rectifier and stripper and small changes therein
p	- Laplace variable for transforms w.r.t. τ
s	- Laplace variable for transforms w.r.t. n
M,m	- liquid hold-up on stages and small change
τ_ℓ	- hydraulic time constant
T_x	- $\bar{M}/L_r$ (or $\bar{M}'/L_s$); time constant
T_ℓ	- τ_ℓ / T_x
$V_r (=V), V_s, v$	- molar flow of vapour in rectifier and stripper and small changes therein
X,X'	- liquid compositions (mal.fraction) in rectifier and stripper
x,x'	- small changes in X and X'
$\bar{X}, \bar{X}'$	- average value of X and X'
X_F	- feed liquid composition
Y,Y'	- vapour composition in rectifier and stripper
y,y'	- small changes in Y and Y'
Y_F	- feed vapour composition

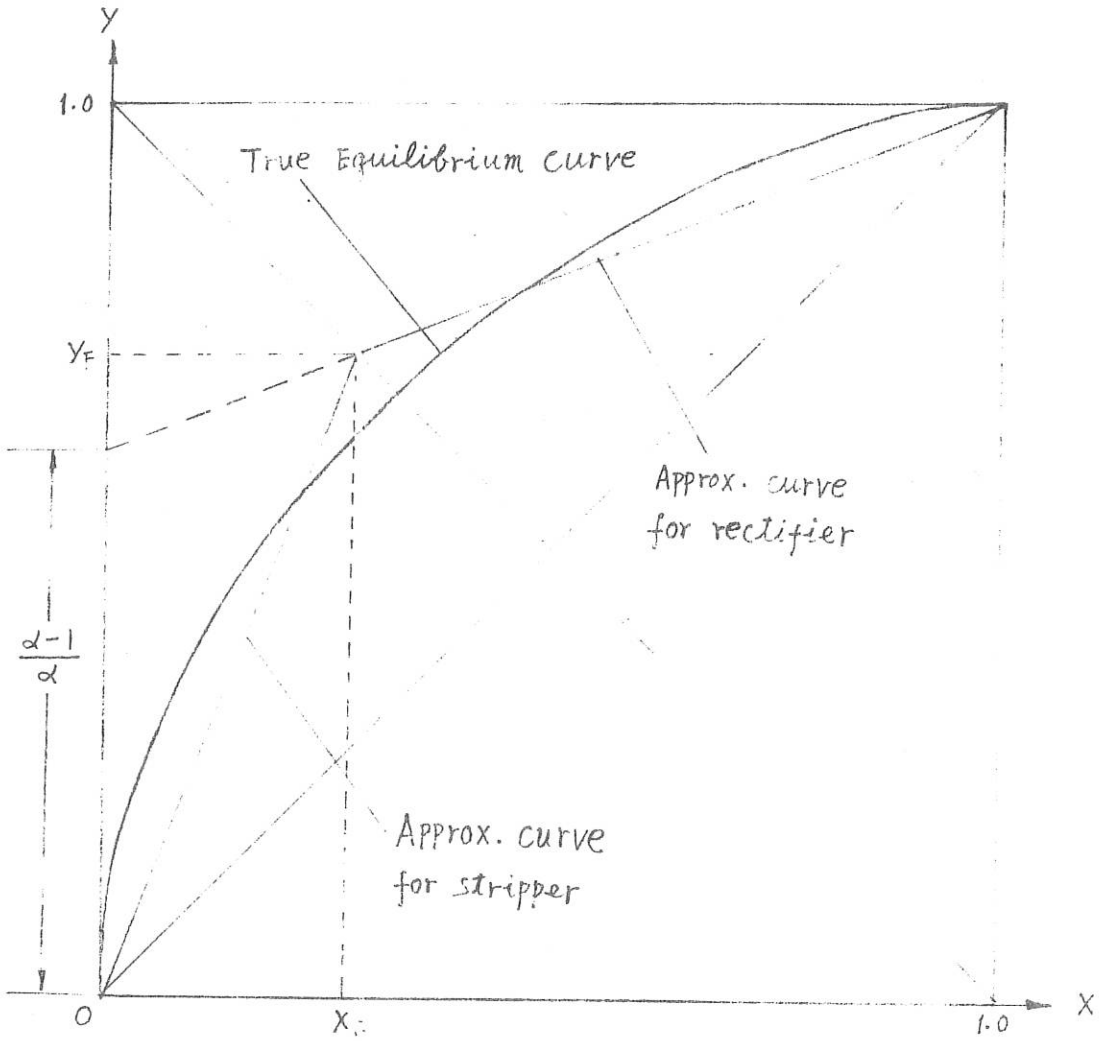

Fig. 1 Vapour / Liquid Equilibrium curve and its piecewise linear approximation

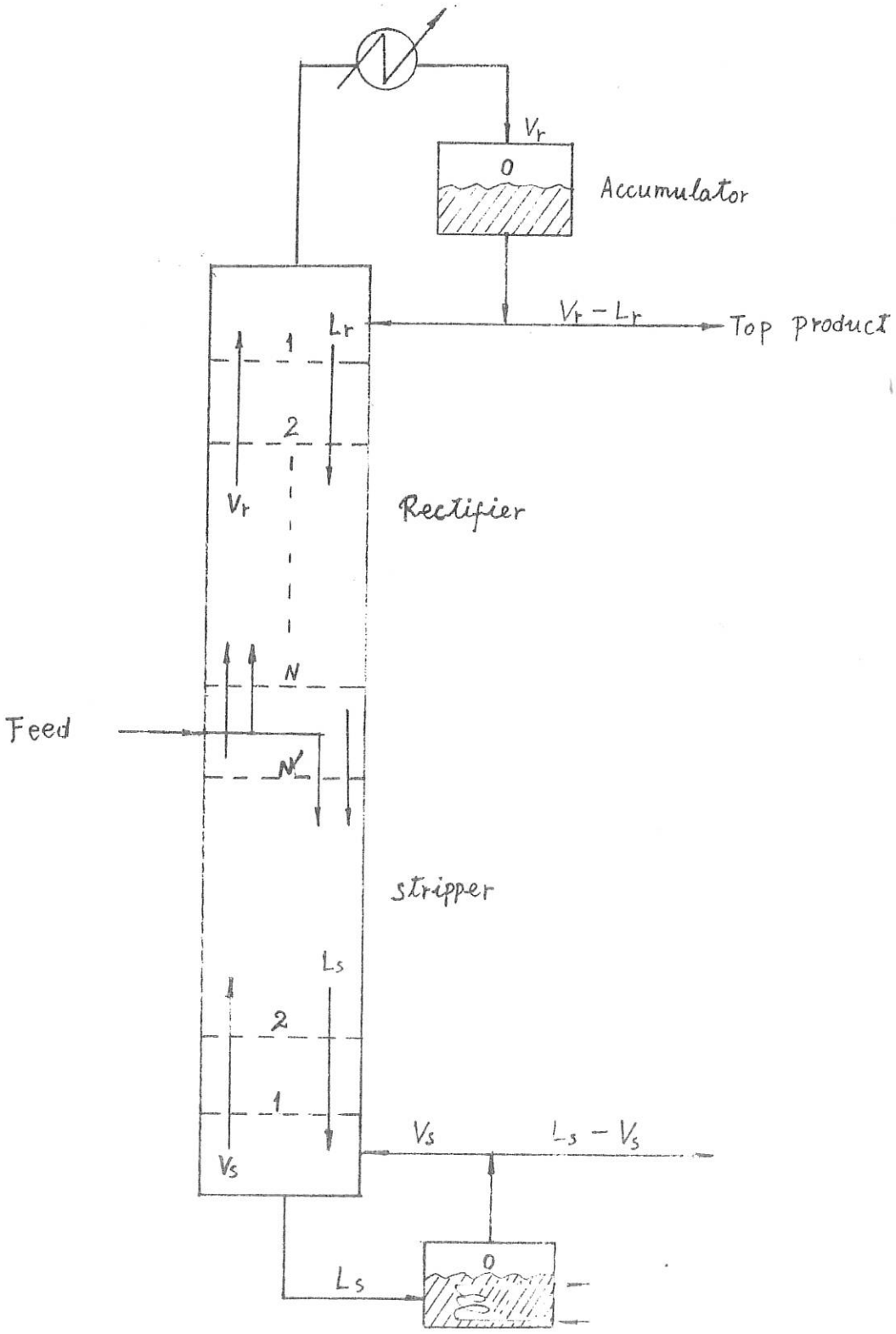

Fig. 2 Illustration of Distillation Column

Fig. 3 Illustration of Mass Flow Balance

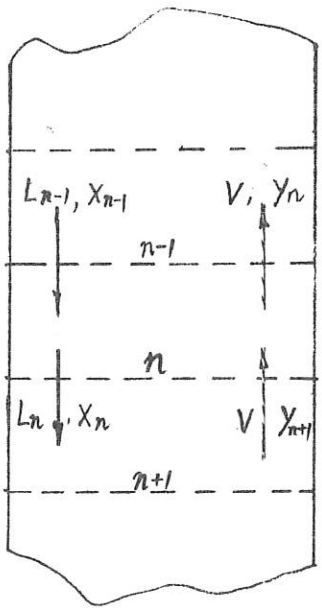

3-1 Mass Flow Balance On n-th stage

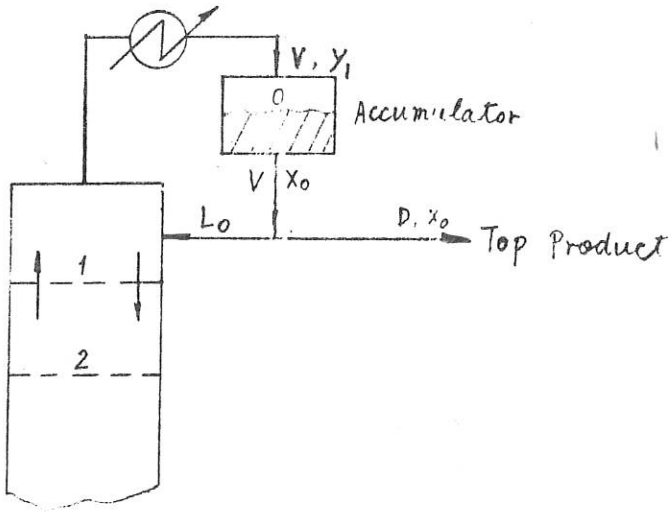

3-2 Mass Flow Balance of Accumulator

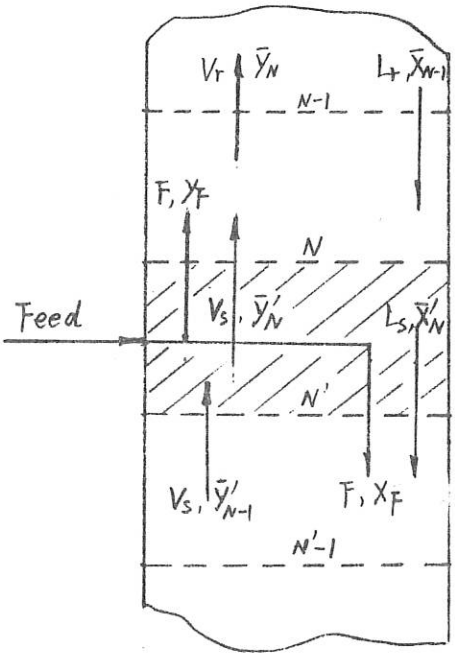

3-2 Mass Flow Balance on Feed stage

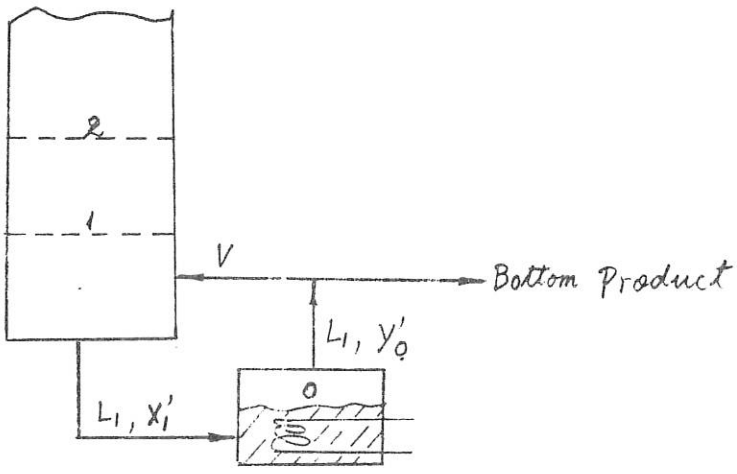

3-4 Mass Flow Balance of Reboiler

BODE DIAGRAM OF G11

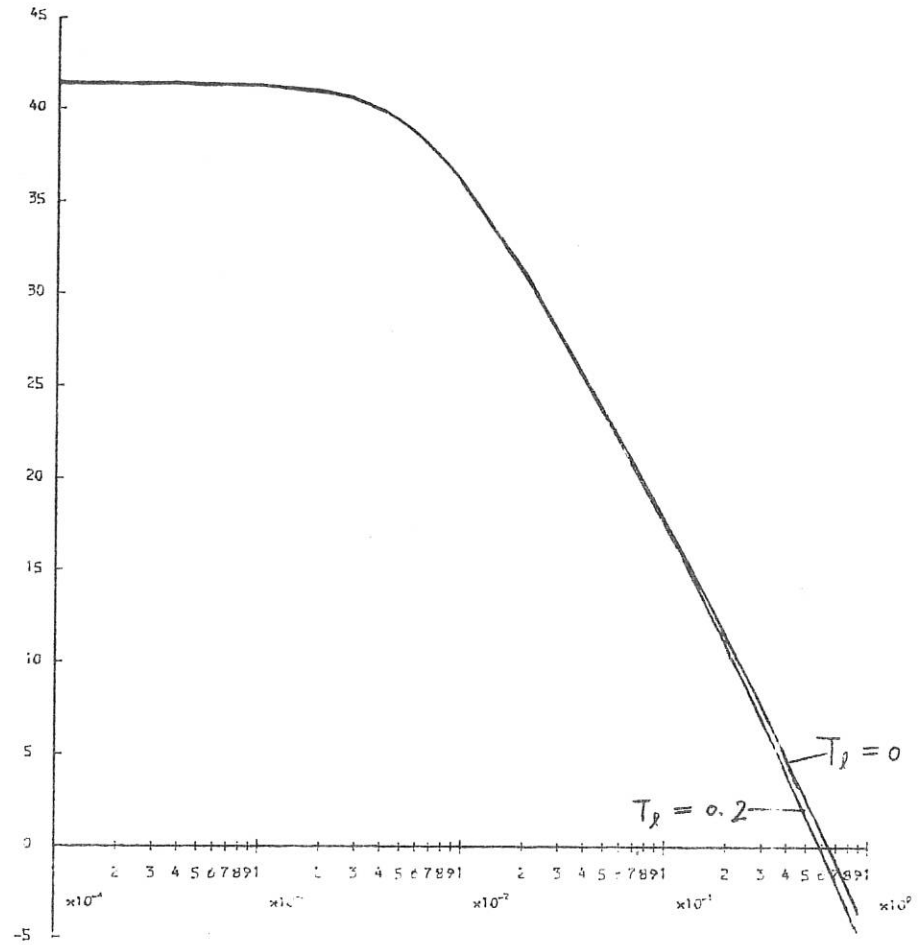

Fig. 4-1

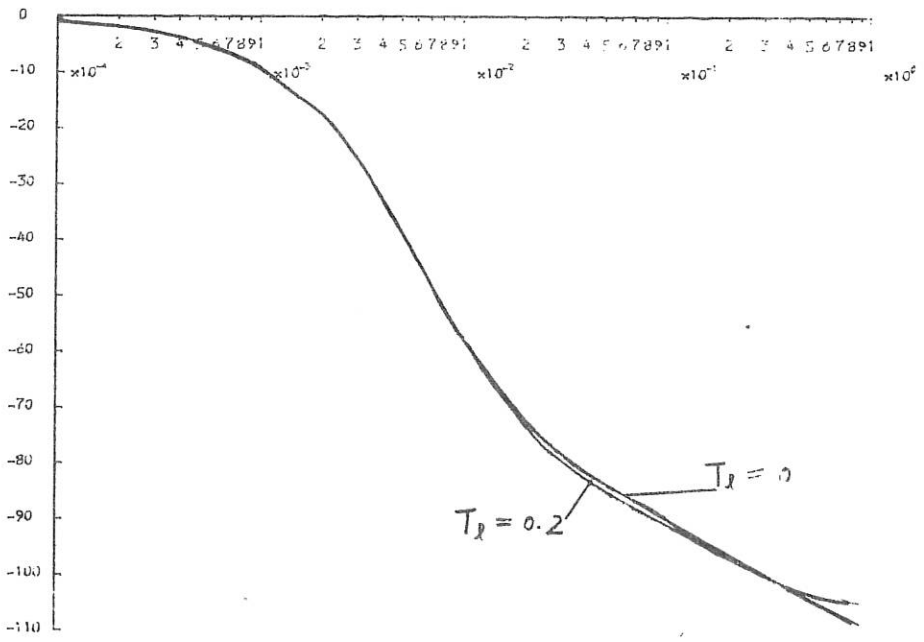

BODE DIAGRAM OF G12

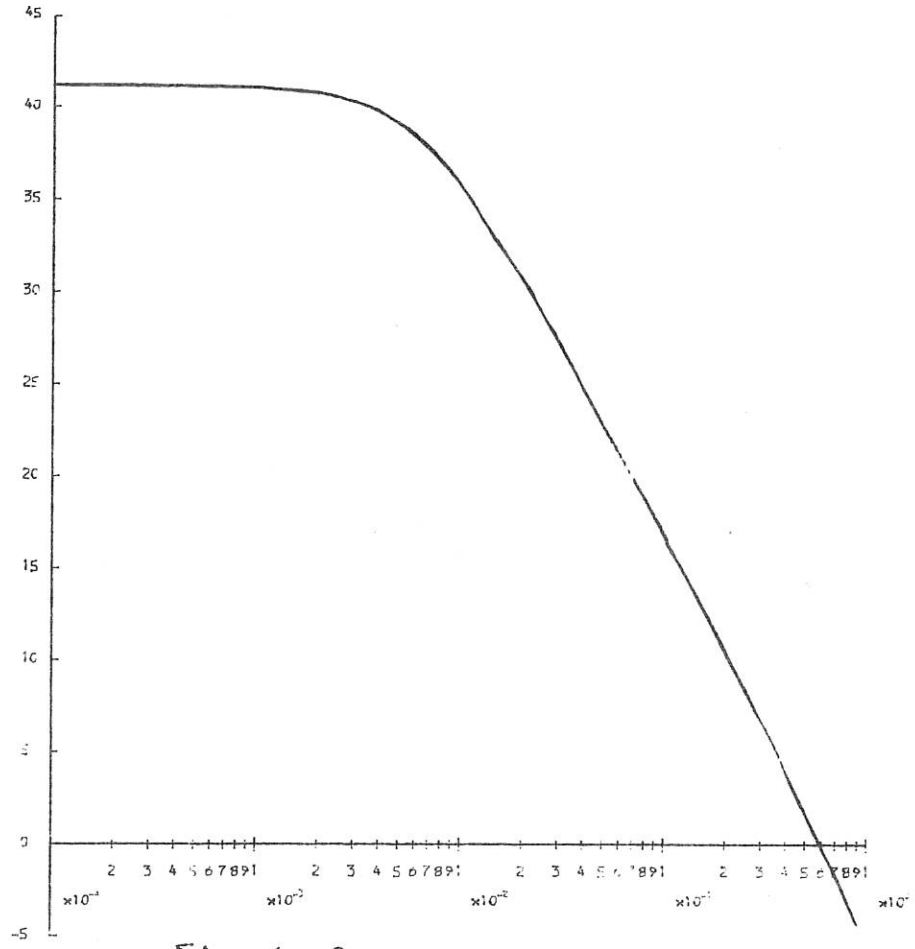

Fig. 4-2

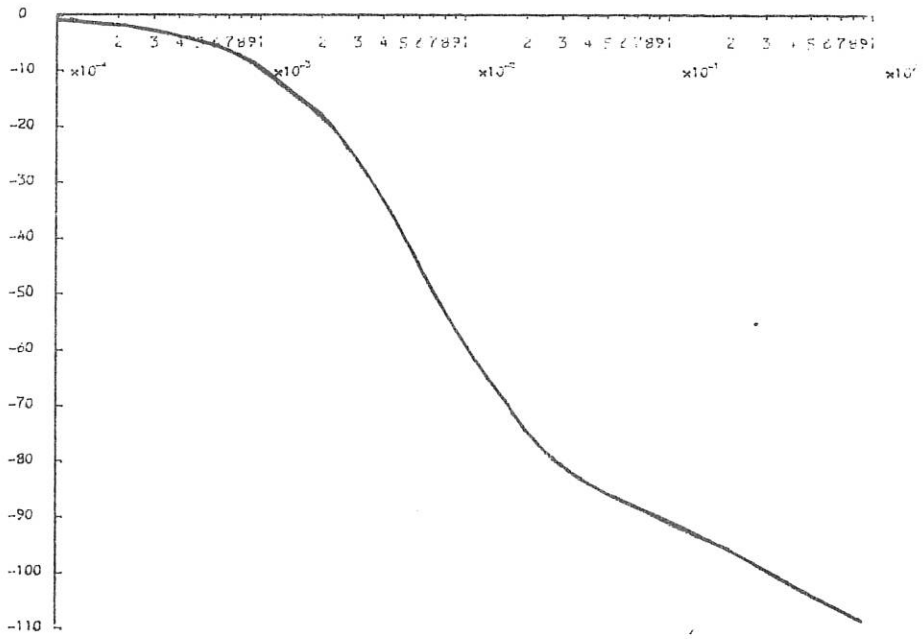

BODE DIAGRAM OF G21

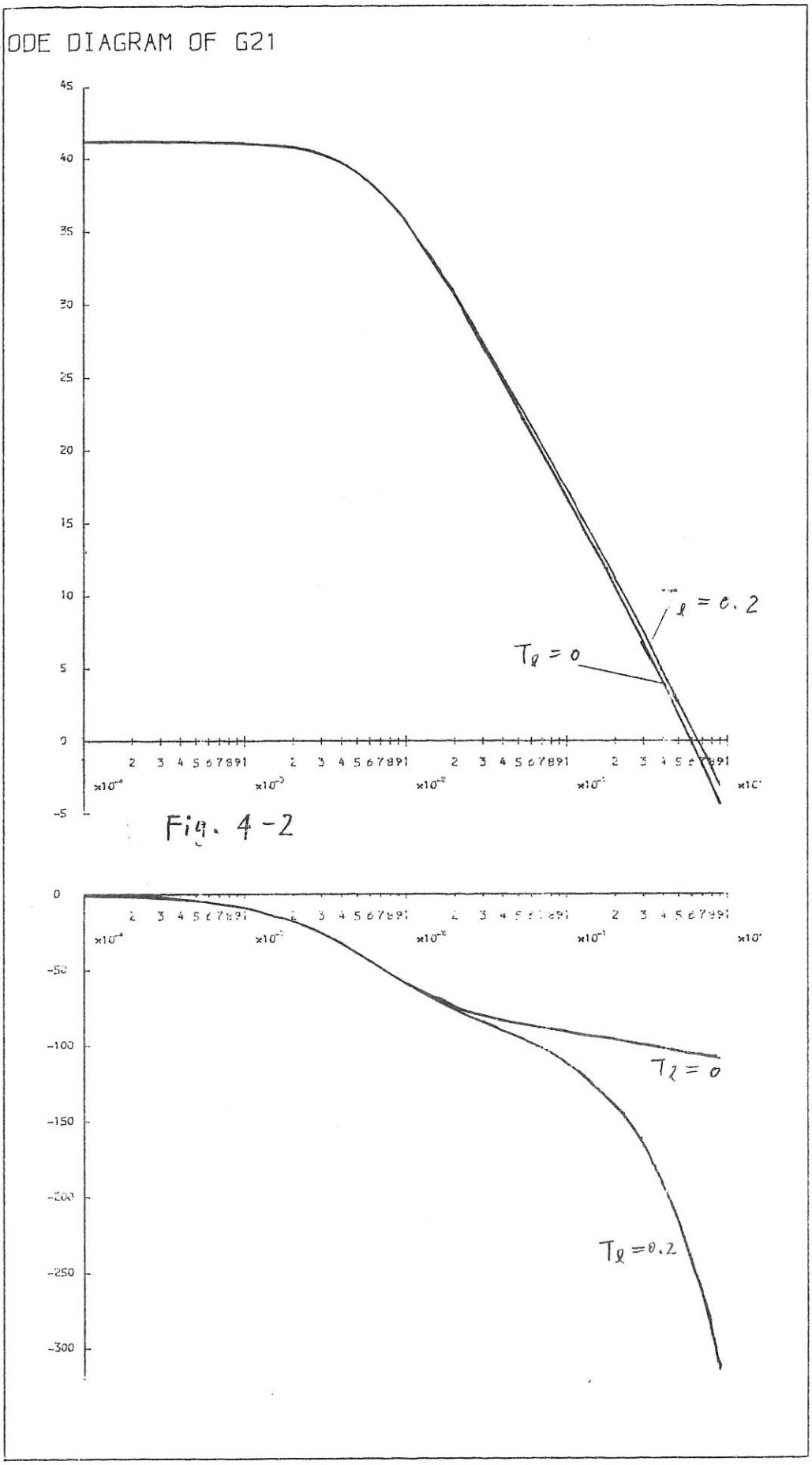

Fig. 4-2

BODE DIAGRAM OF G22

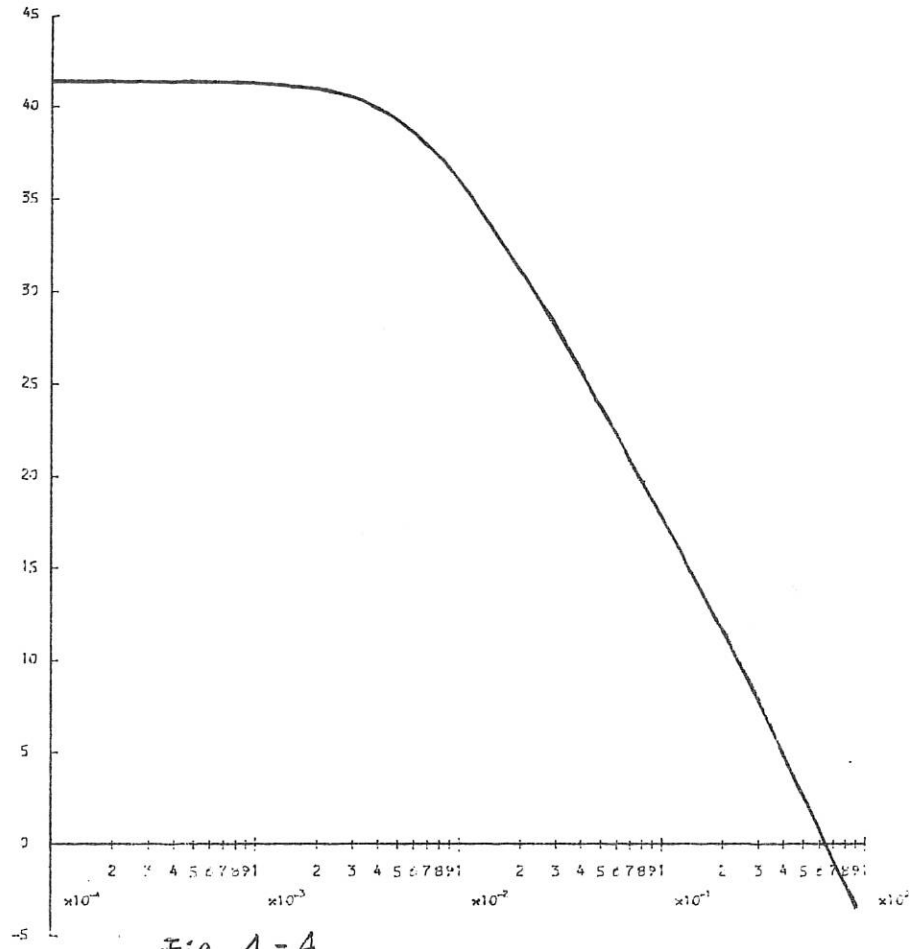

Fig. 4-4

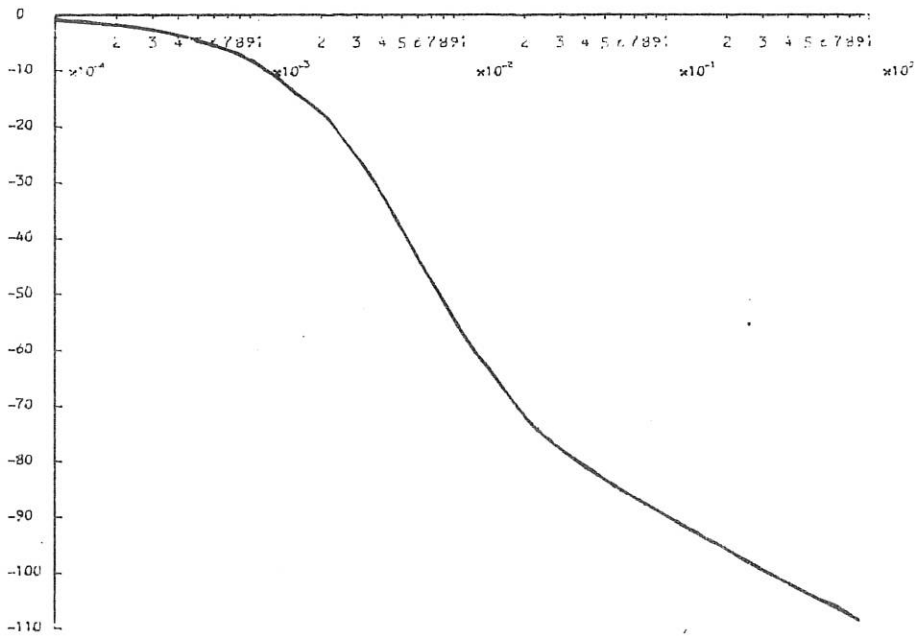

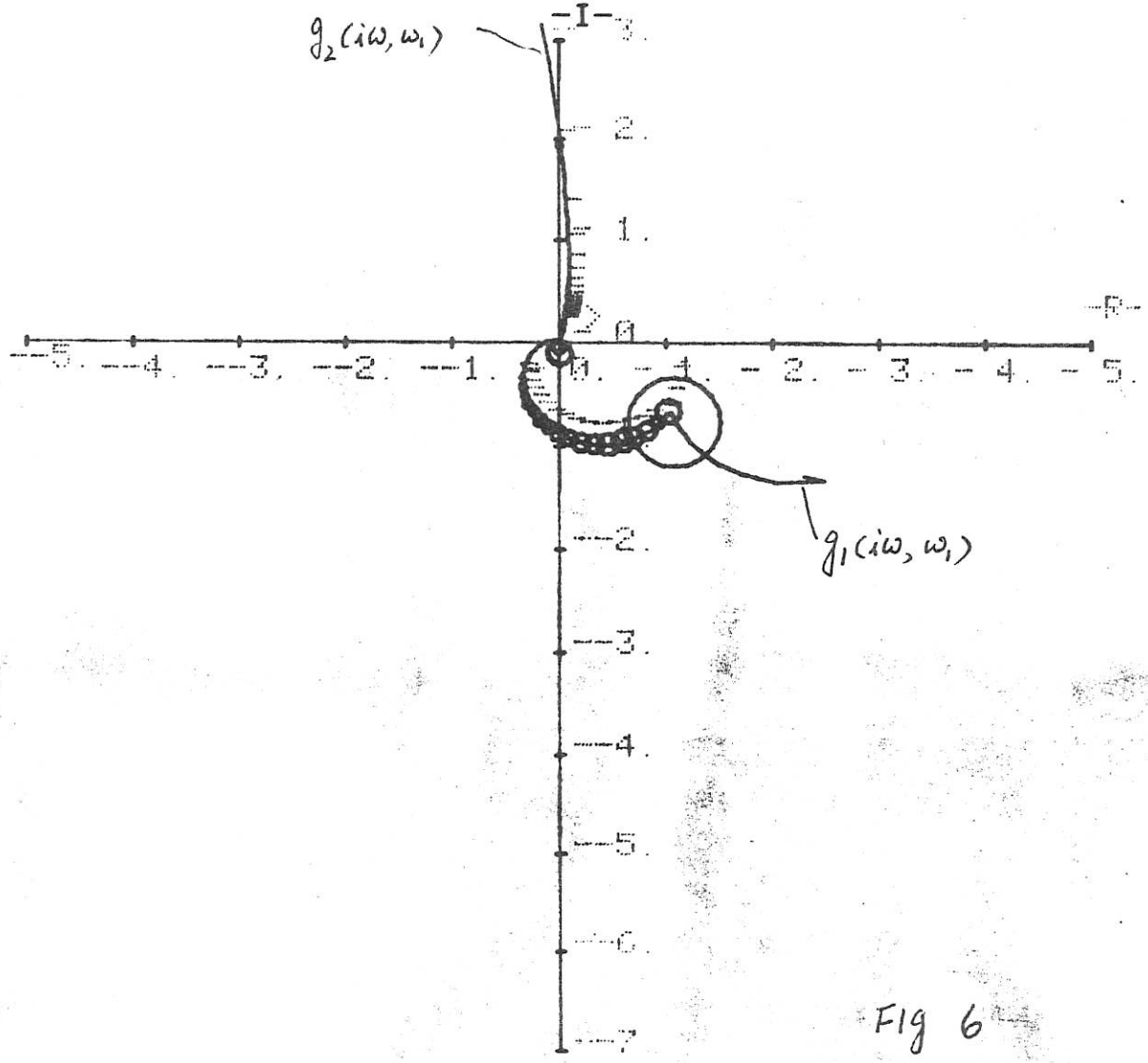

Fig 6

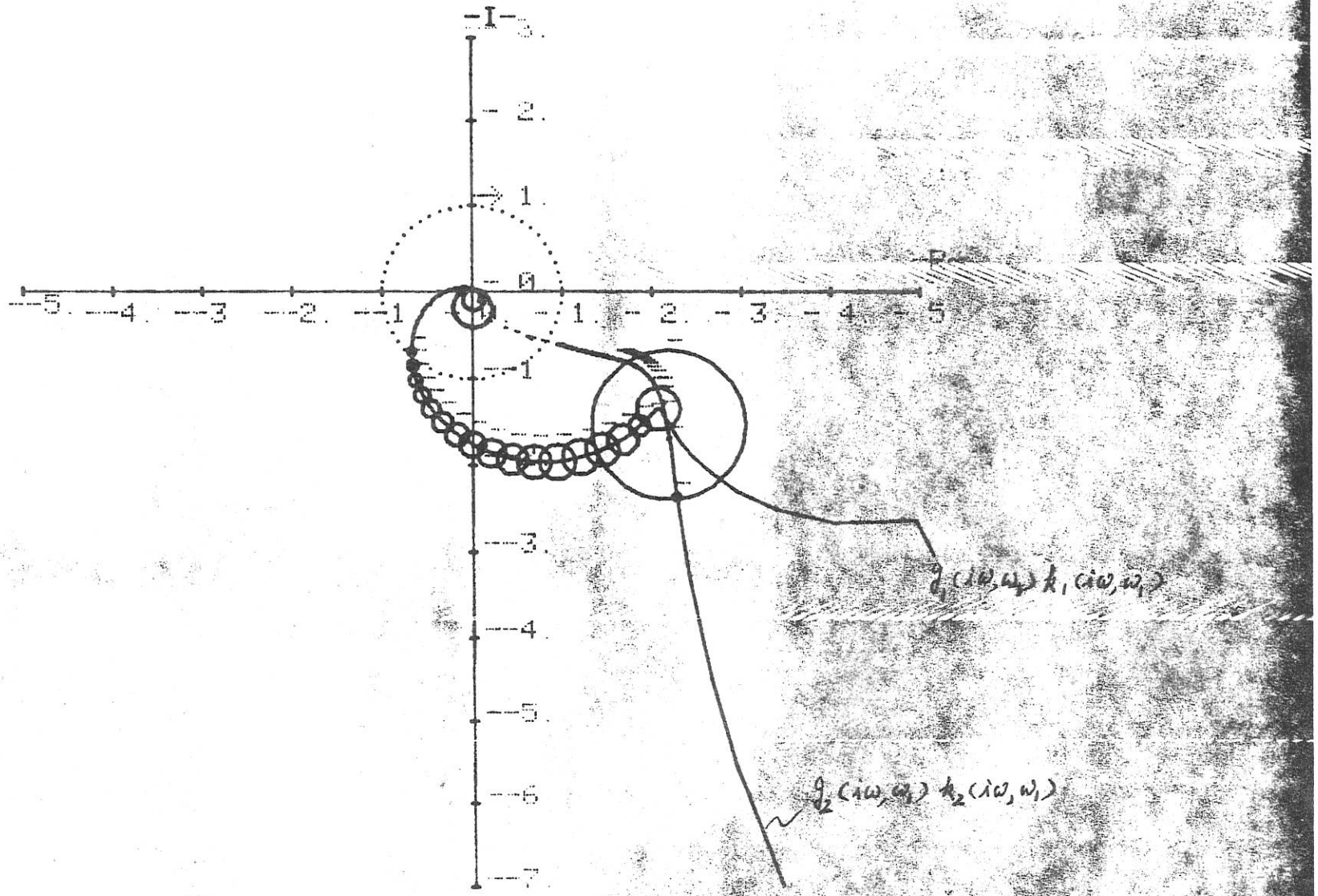
I
3
2
1
0
-1
-2
-3
-4
-5
-6
-7
-5
-4
-3
-2
-1
1
2
3
4
5
R
$g_1(i\omega,\omega_1)\,k_1(i\omega,\omega_1)$
$g_2(i\omega,\omega_1)\,k_2(i\omega,\omega_1)$

Fig 7

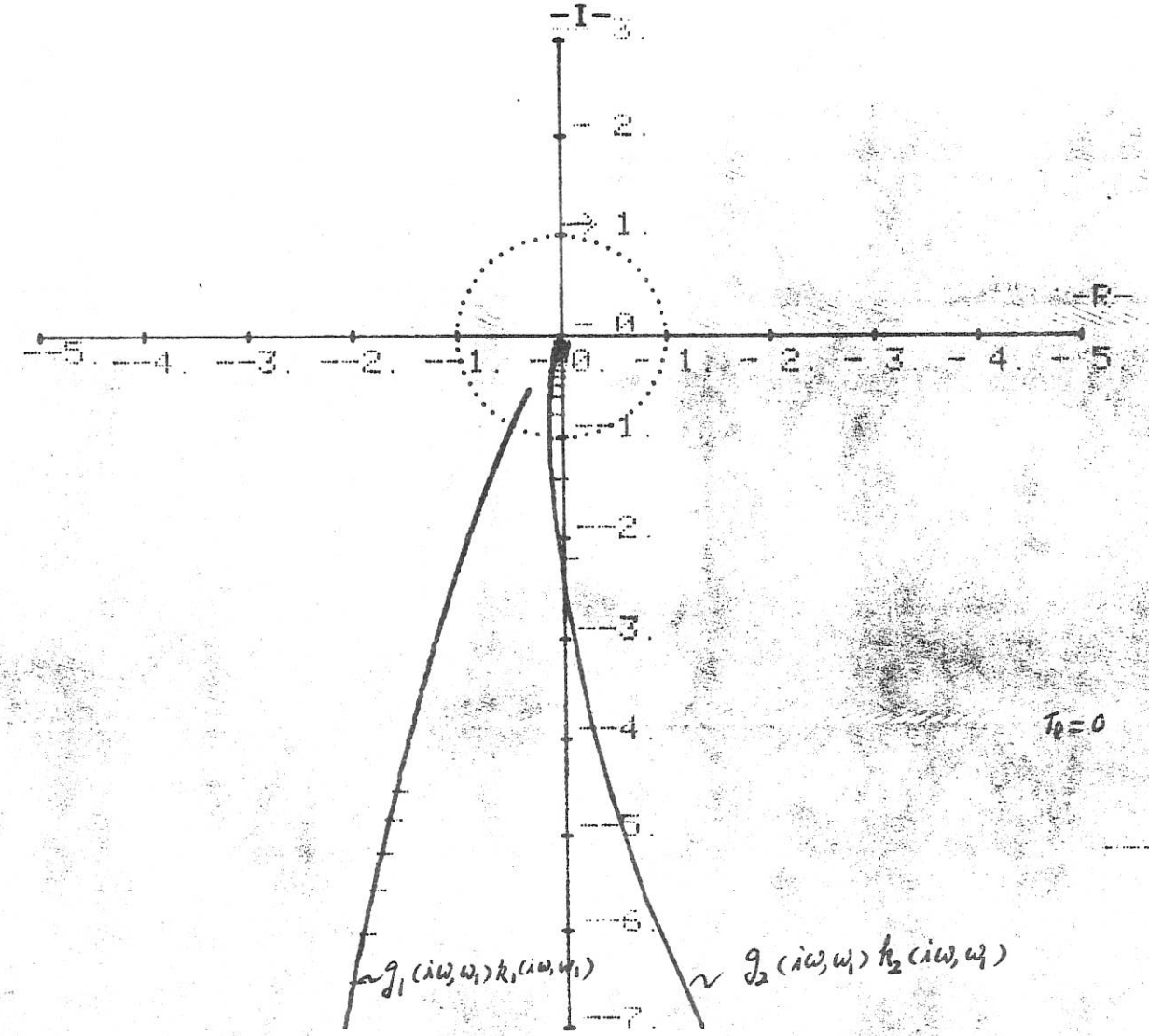
-I-
3.
2.
1.
0
-R-
-5. -4. -3. -2. -1. -0. 1. 2. 3. 4. 5
-1.
-2.
-3.
-4.
-5.
-6.
-7.
$T_0 = 0$
$g_1(i\omega, \omega_1) k_1(i\omega, \omega_1)$
$g_2(i\omega, \omega_1) k_2(i\omega, \omega_1)$

Fig 8

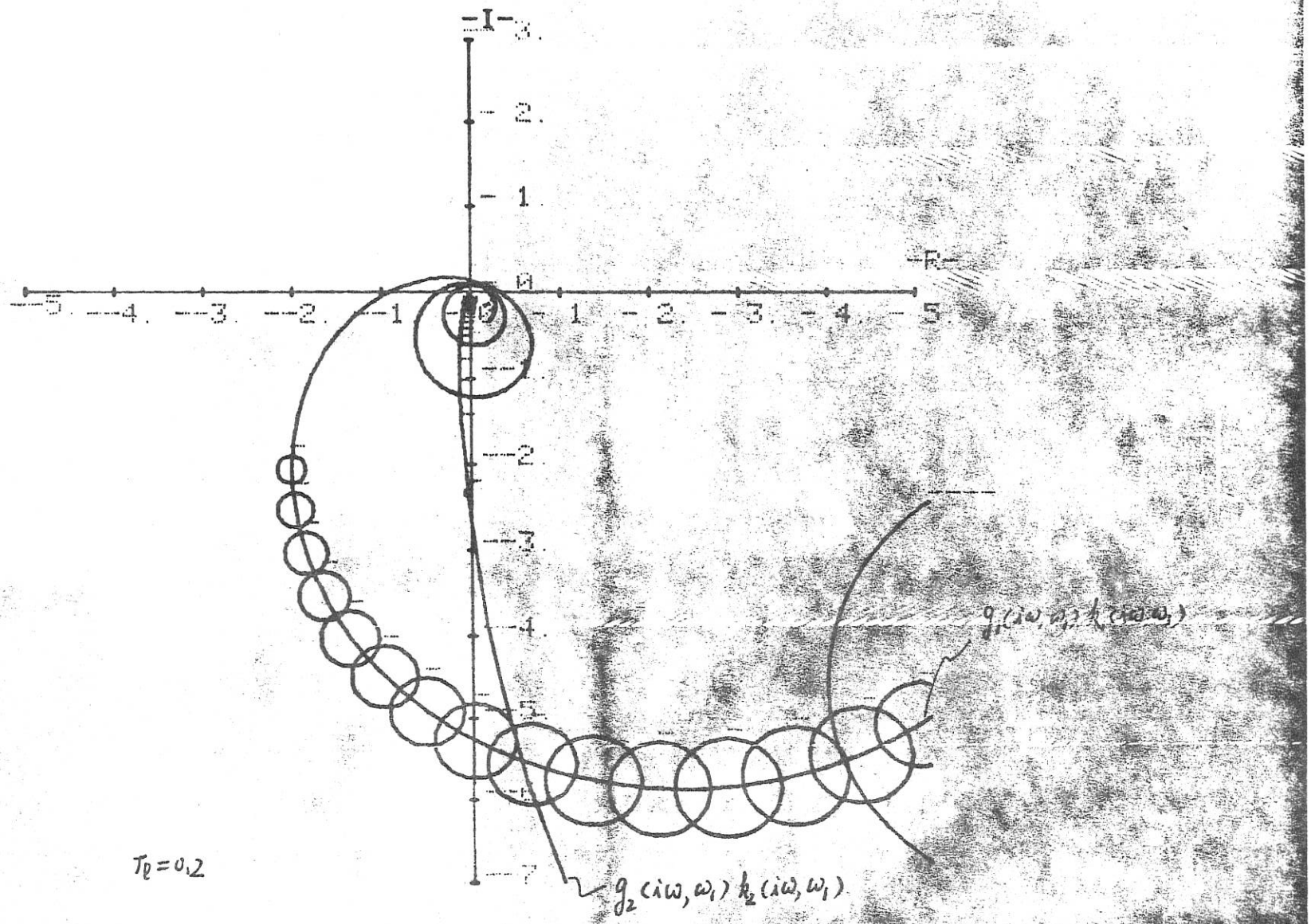
I
R
3
2
1
0
-1
-2
-3
-4
-5
-4
-3
-2
-1
1
2
3
4
5
$T_\ell = 0,2$
$g_1(i\omega,\omega_1)\,k_1(i\omega,\omega_1)$
$g_2(i\omega,\omega_1)\,k_2(i\omega,\omega_1)$

Fig 9

DIAGRAMS FOR RESEARCH REPORT NO. 209

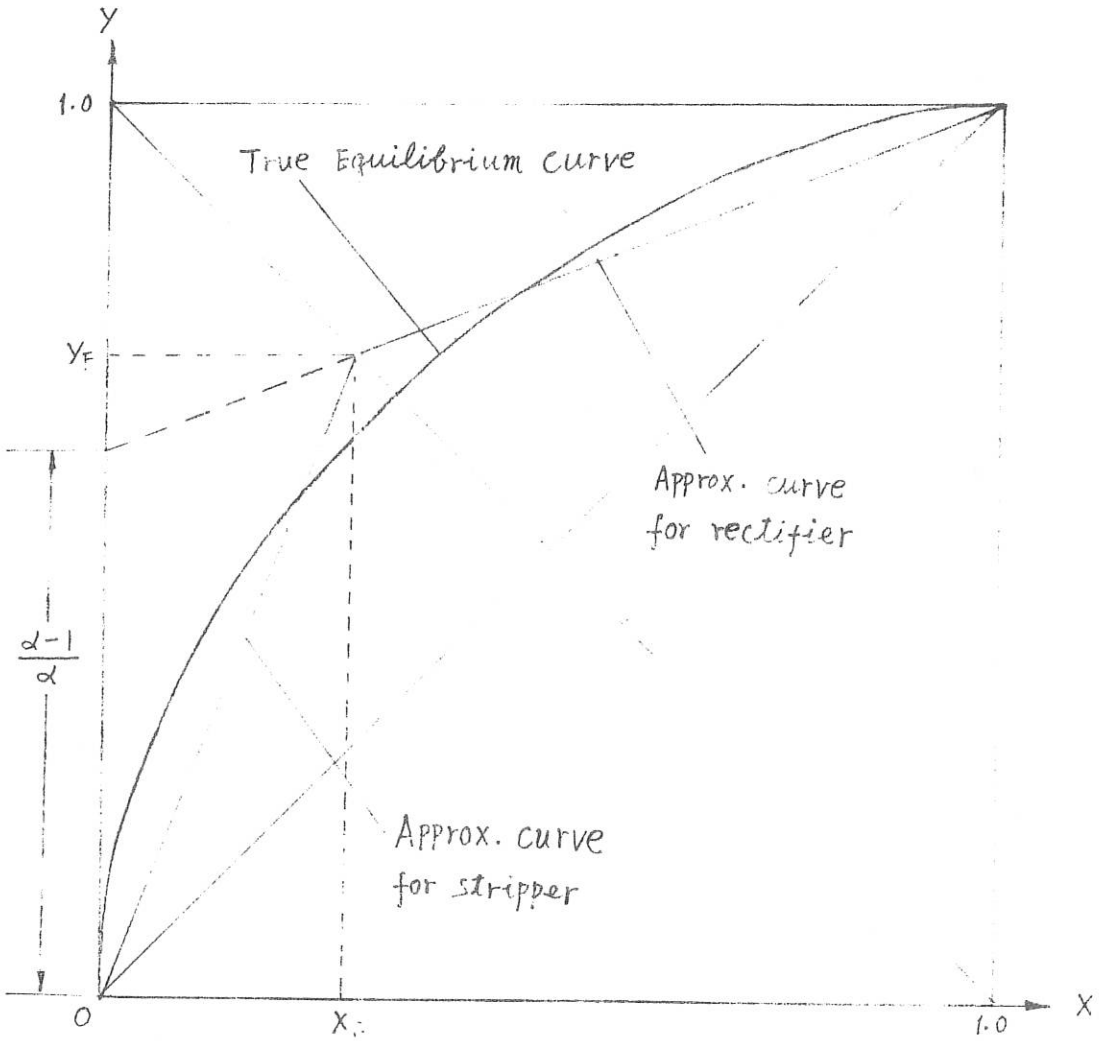

Fig. 1 Vapour / Liquid Equilibrium curve and its piecewise linear approximation

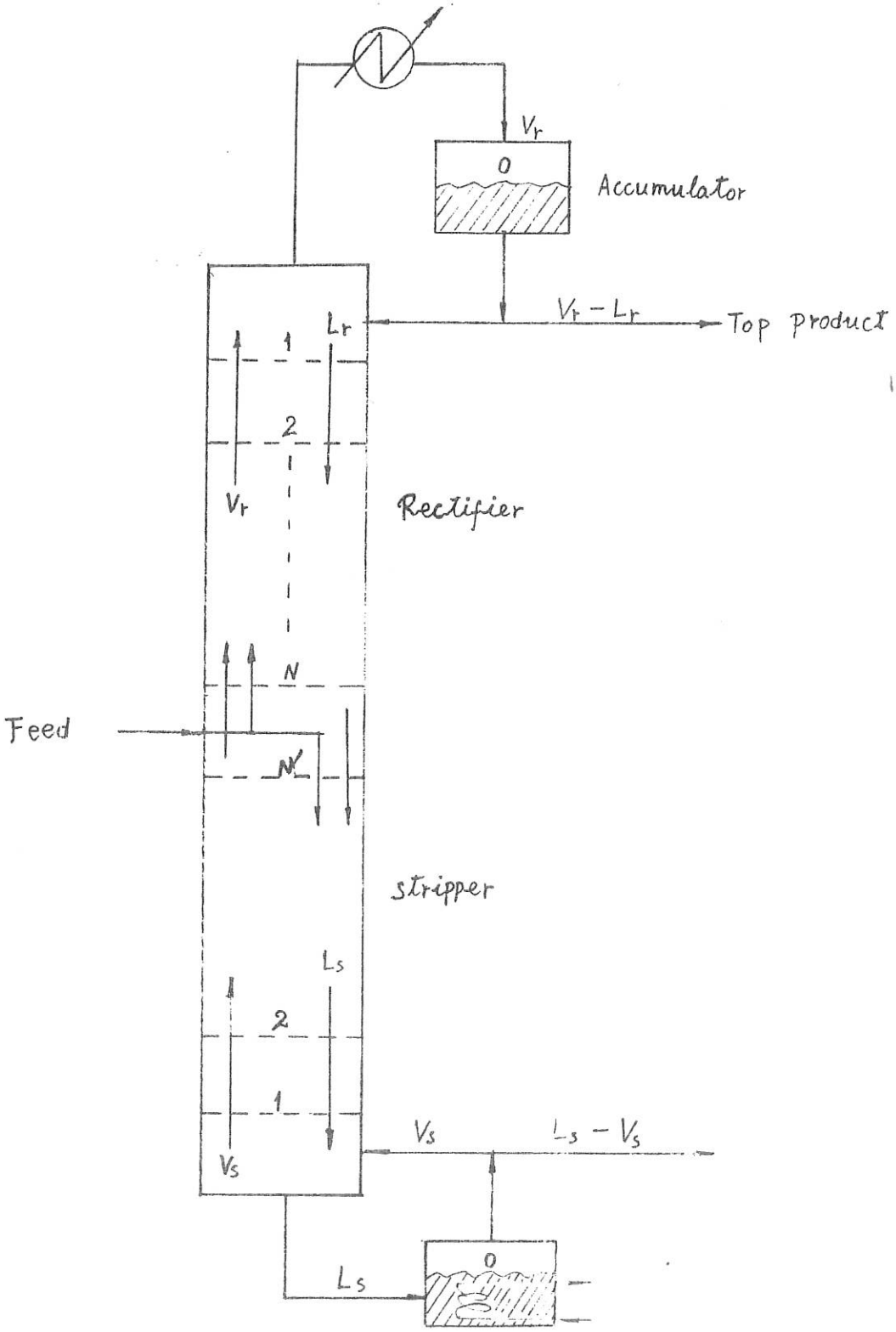

Fig. 2 Illustration of Distillation Column

Fig. 3 Illustration of Mass Flow Balance

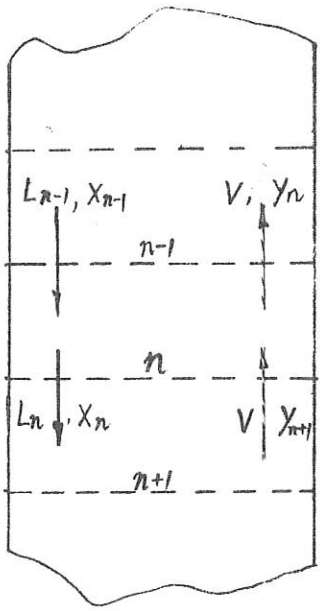

3-1 Mass Flow Balance On n-th stage

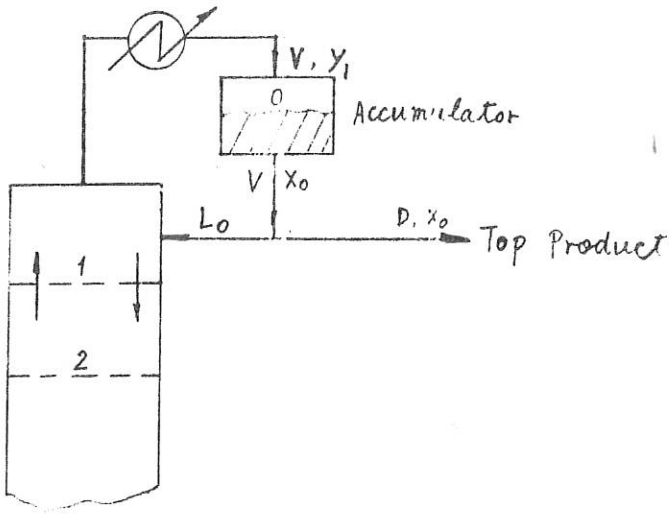

3-2 Mass Flow Balance of Accumulator

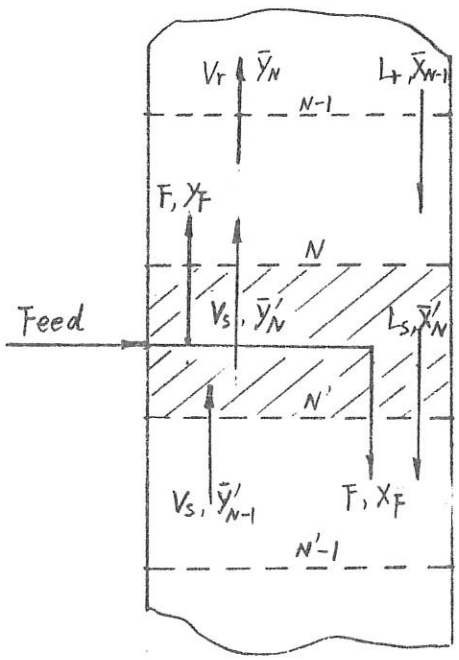

3-2 Mass Flow Balance on Feed stage

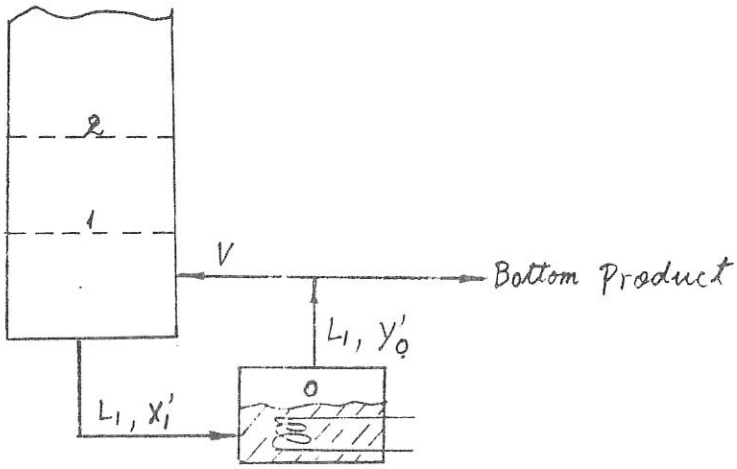

3-4 Mass Flow Balance of Reboiler

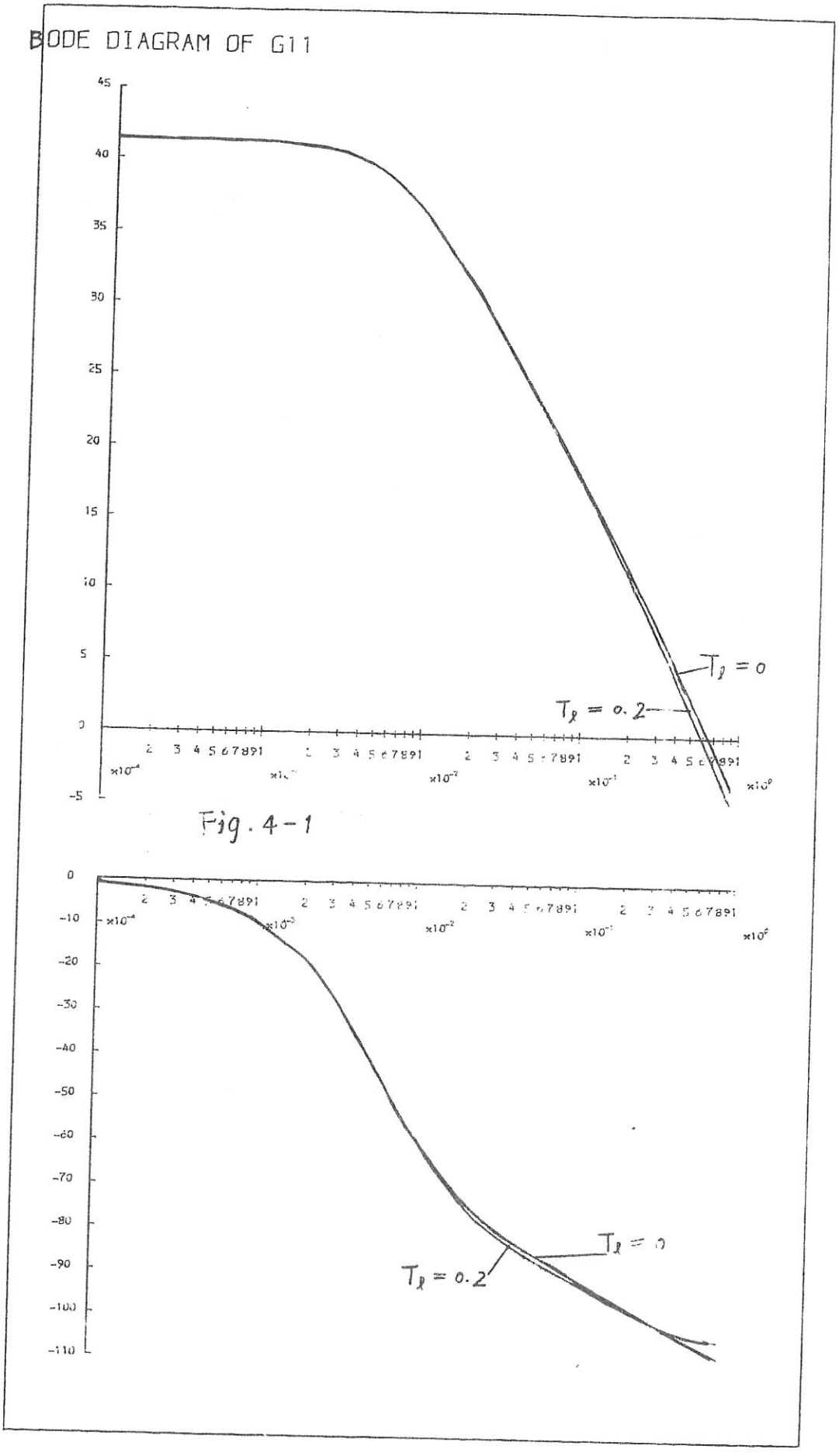
BODE DIAGRAM OF G11
45
40
35
30
25
20
15
10
5
0
-5
$T_d = 0$
$T_d = 0.2$
0
-10
-20
-30
-40
-50
-60
-70
-80
-90
-100
-110
$T_d = 0$
$T_d = 0.2$

Fig. 4-1

BODE DIAGRAM OF G12

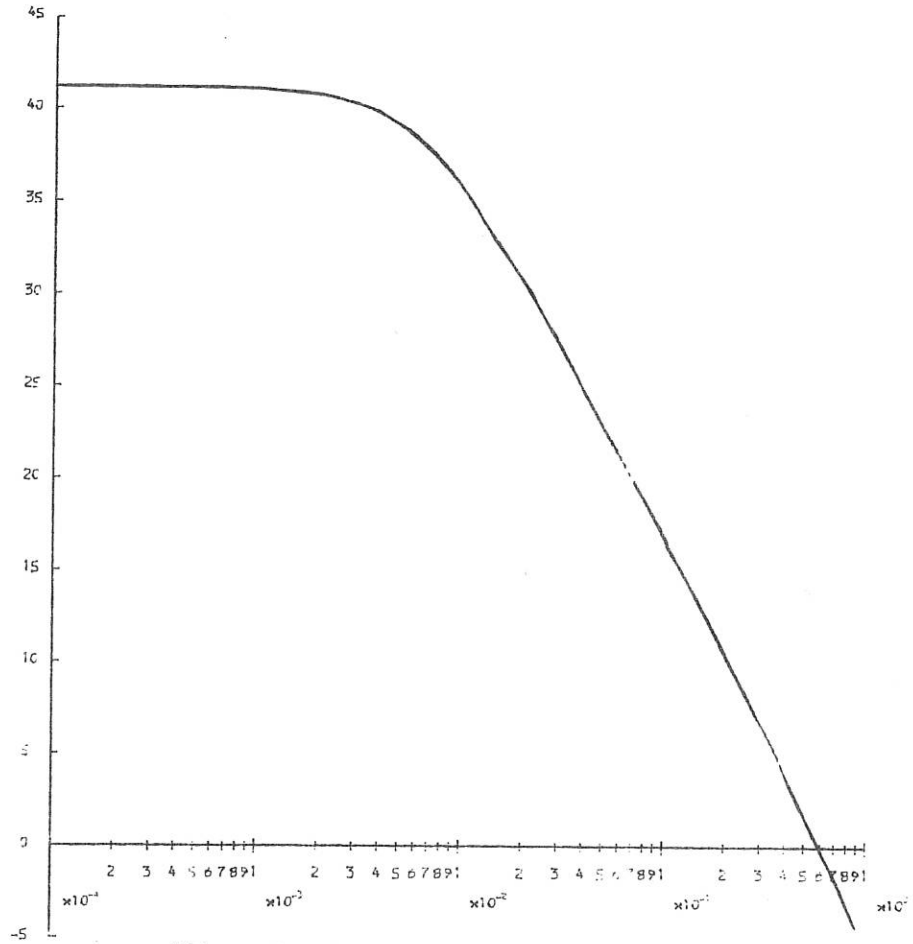

Fig. 4-2

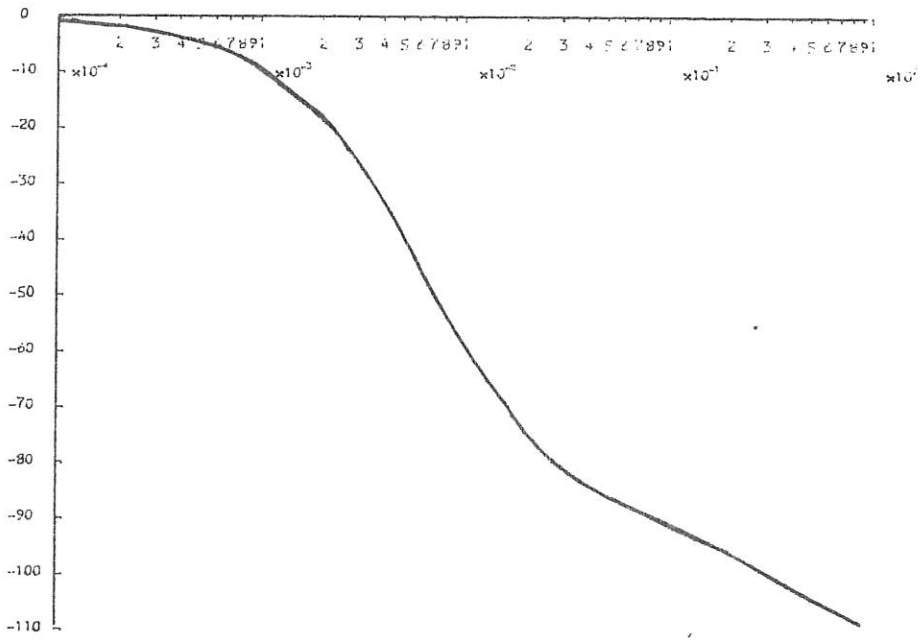

BODE DIAGRAM OF G21

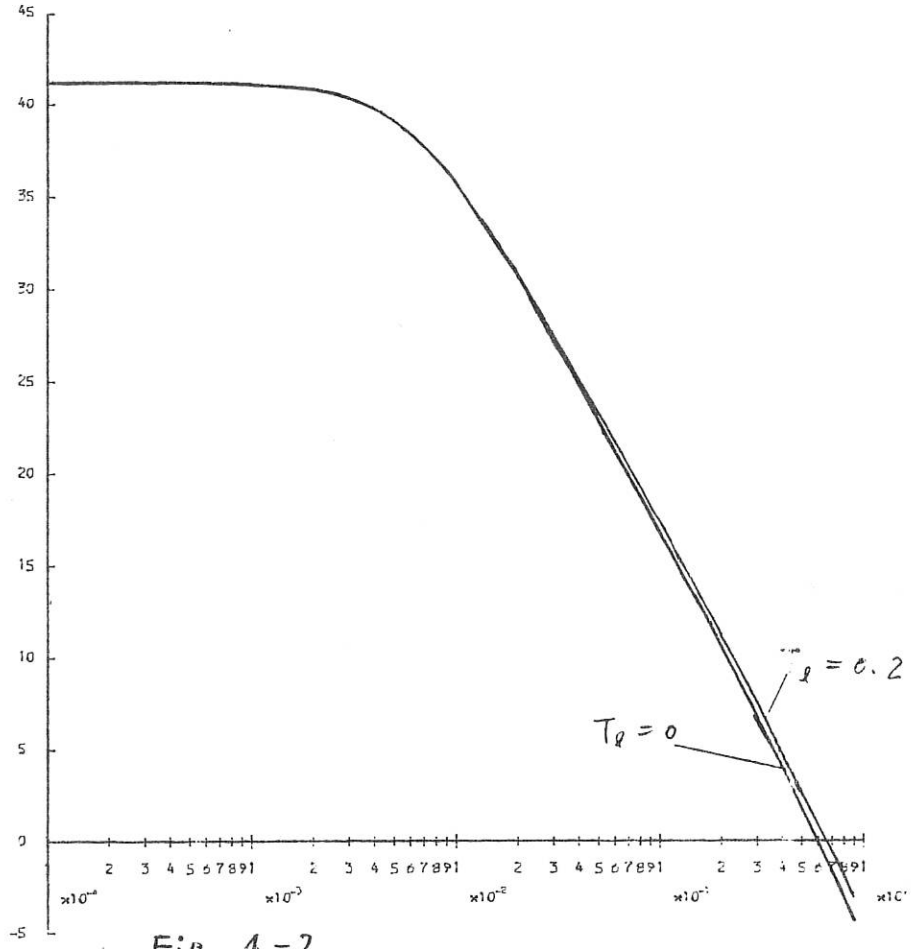

Fig. 4-2

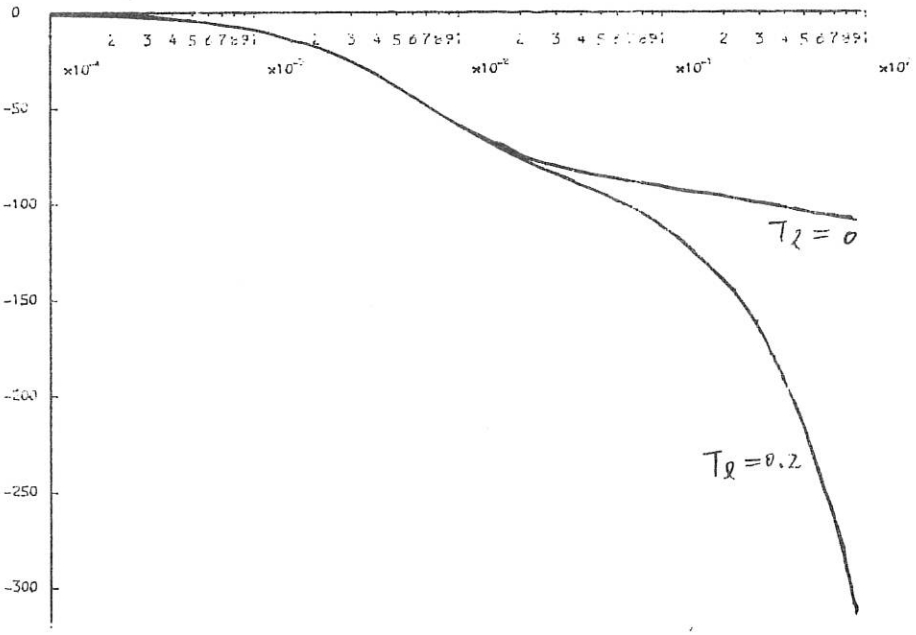

BODE DIAGRAM OF G22

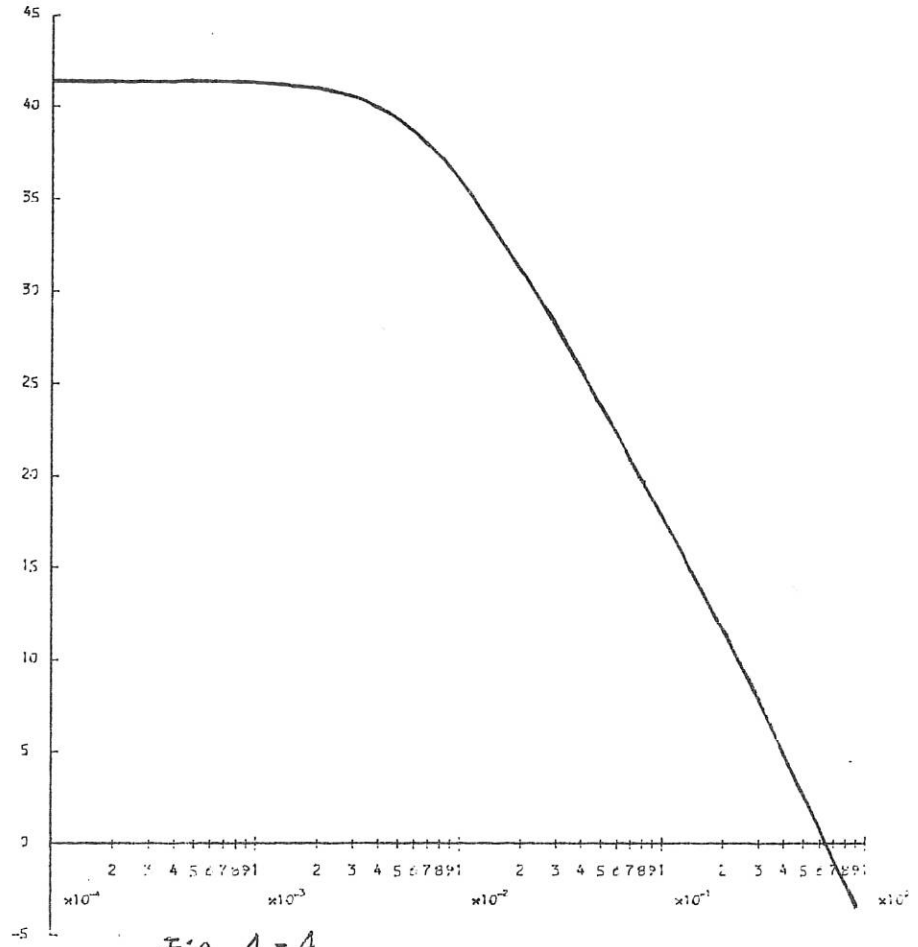

Fig. 4-4

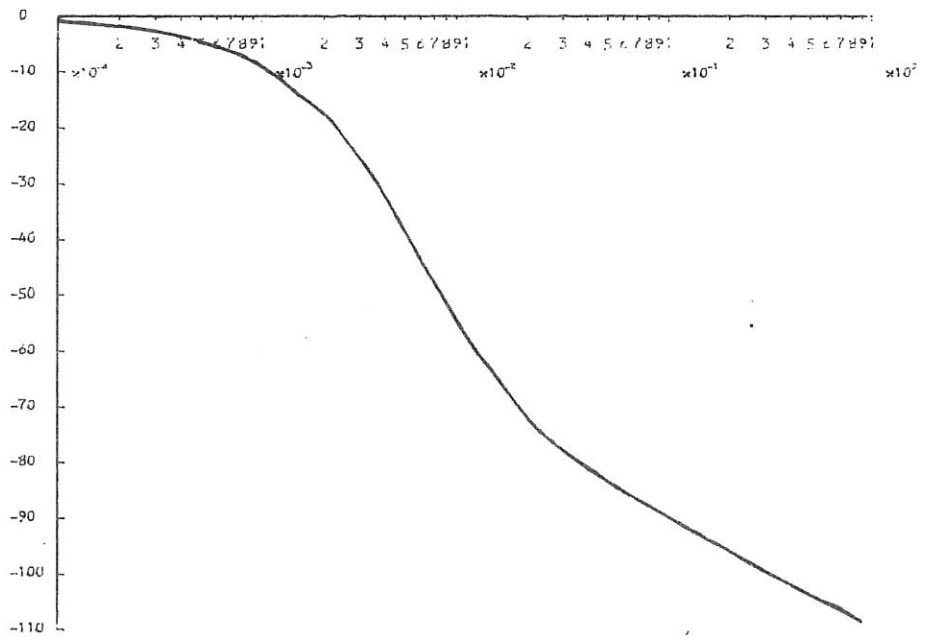

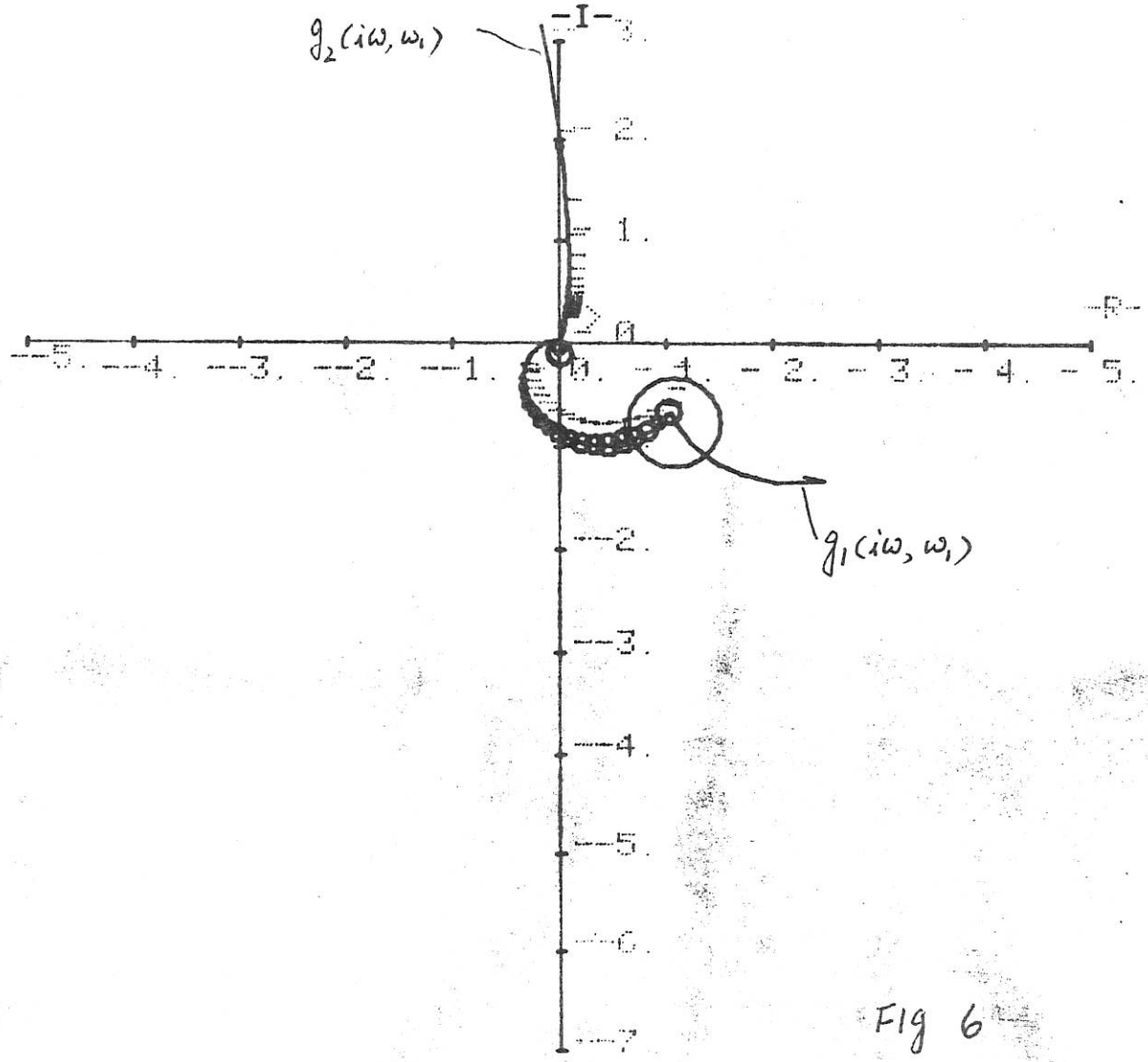

Fig 6

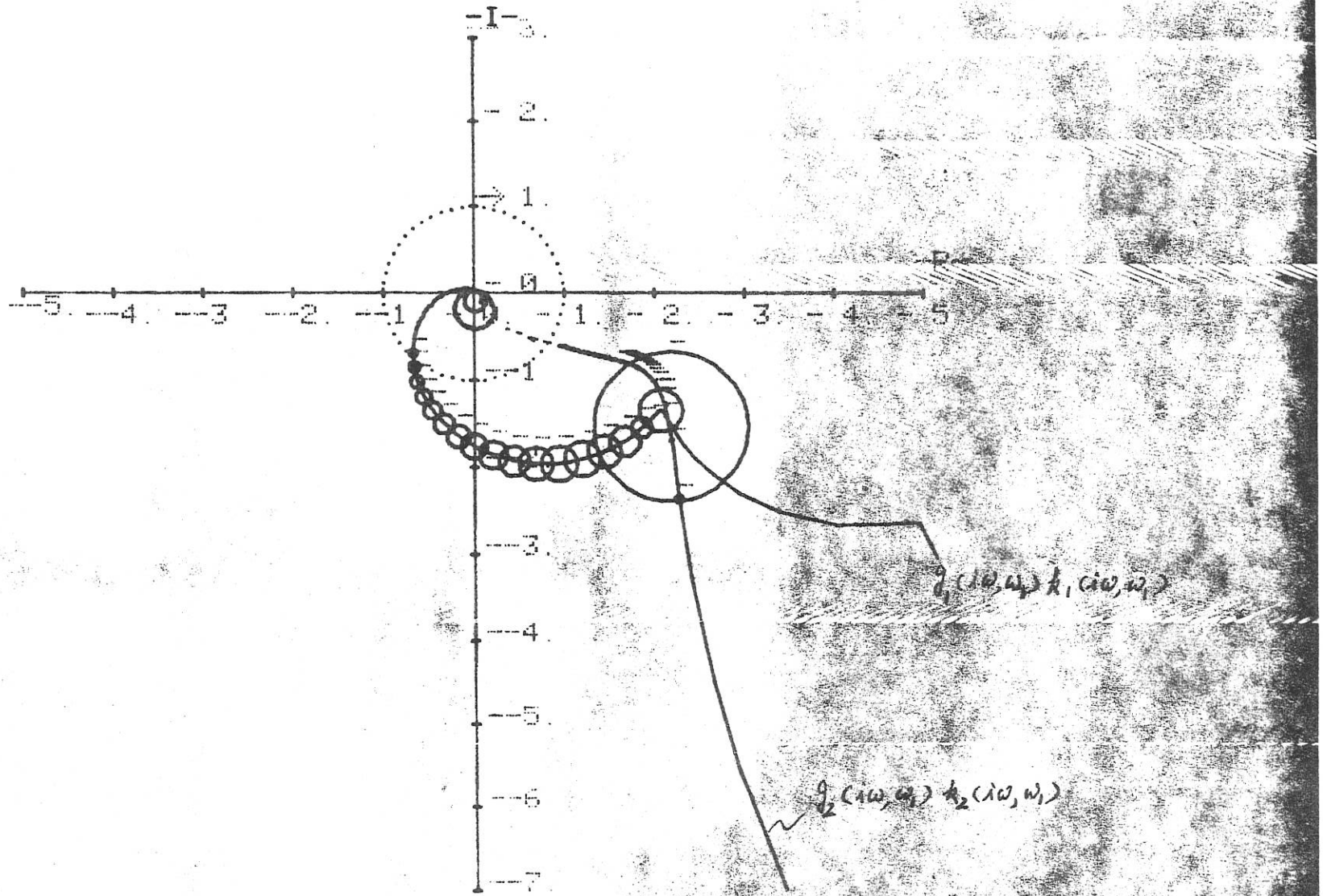
I
2
1
0
-1
-3
-4
-5
-6
-7
-5
-4
-3
-2
-1
1
2
3
4
5
R
$g_1(i\omega,\omega_1)\,k_1(i\omega,\omega_1)$
$g_2(i\omega,\omega_1)\,k_2(i\omega,\omega_1)$

Fig 7

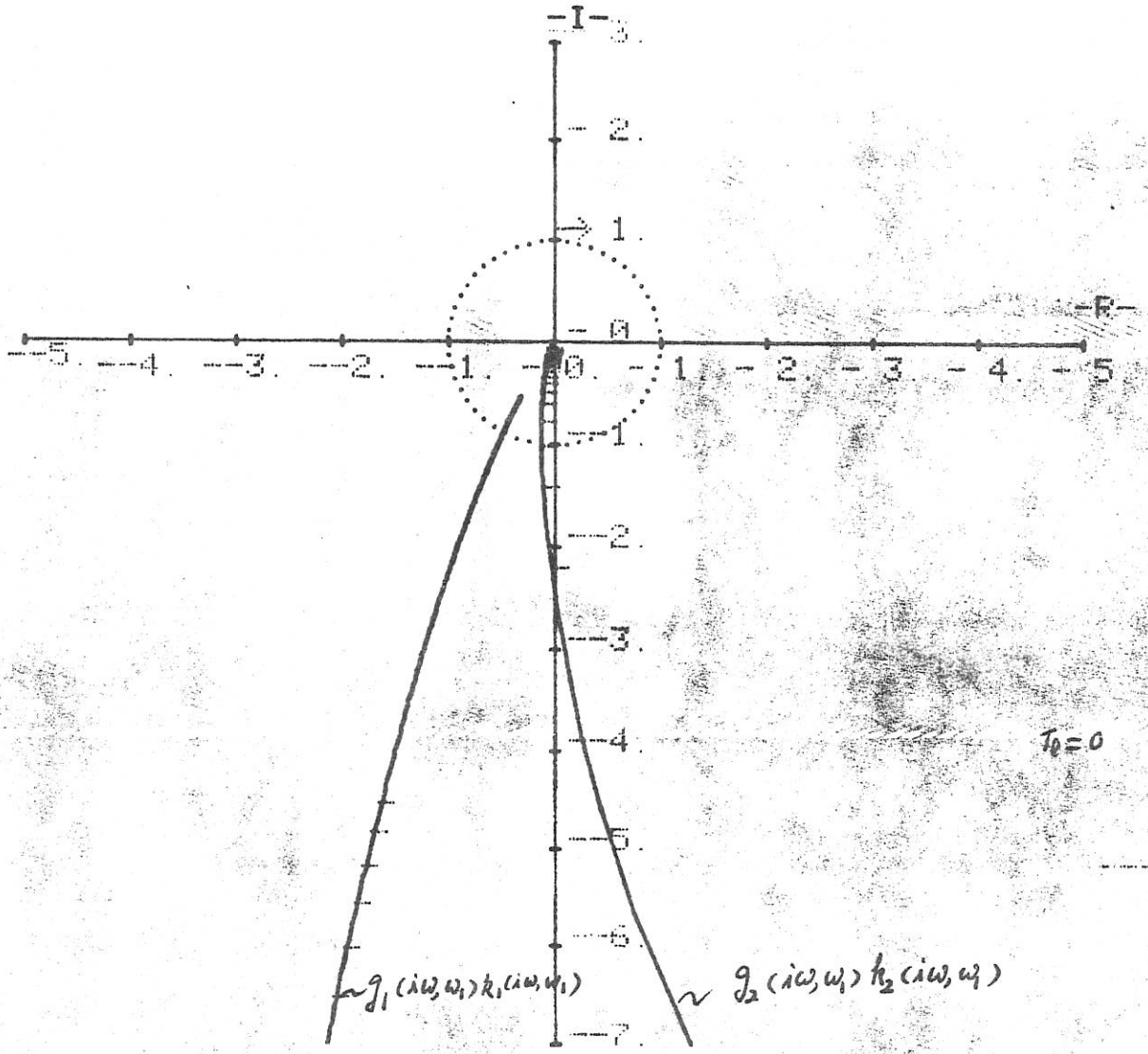
-I-
3.
2.
1.
0.
-1.
-2.
-3.
-4.
-5.
-6.
-7.
-R-
-5.
-4.
-3.
-2.
-1.
0.
1.
2.
3.
4.
5.
$T_0 = 0$
$g_1(i\omega, \omega_1) k_1(i\omega, \omega_1)$
$g_2(i\omega, \omega_1) k_2(i\omega, \omega_1)$

Fig 8

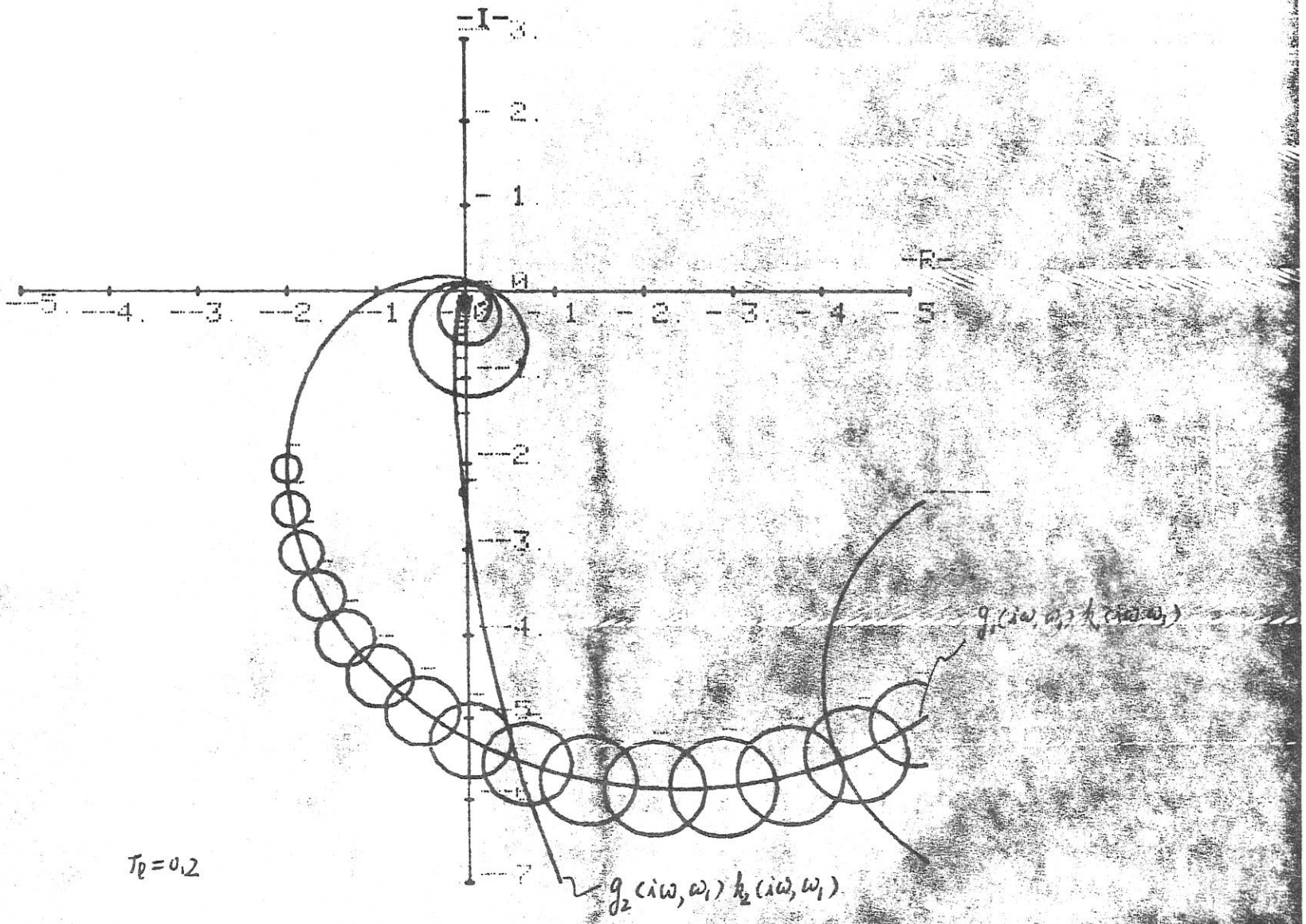
-I-
3.
2.
1.
-R-
-5.
-4.
-3.
-2.
-1.
0
1.
2.
3.
4.
5.
-2.
-3.
-4.
-5.
-7.
$q_1(i\omega,\omega_1)\,k_1(i\omega,\omega_1)$
$q_2(i\omega,\omega_1)\,k_2(i\omega,\omega_1)$
$T_0 = 0{,}2$

Fig 9